Antioxidants & Redox Signalling – invited Forum Review Article (April 2017)

Redox-sensing iron-sulfur cluster regulators

Jason C. Crack and Nick E Le Brun[1]

Centre for Molecular and Structural Biochemistry, School of Chemistry, University of East Anglia, Norwich Research Park, Norwich NR4 7TJ, UK

[1]Address correspondence to: Nick E Le Brun, School of Chemistry, University of East Anglia, Norwich NR4 7TJ, UK. Tel. +44 1603 592699; Fax. +44 1603 592003; Email: n.le-brun@uea.ac.uk

Word count: 9101

Number of references: 187

Number of colour illustrations: 9

Abstract

Significance. Iron-sulfur cluster proteins carry out a wide range of functions, including as regulators of gene transcription/translation in response to environmental stimuli. In all known cases, the cluster acts as the sensory module, where the inherent reactivity/fragility of iron-sulfur clusters towards small/redox active molecules is exploited to effect conformational changes that modulate binding to DNA regulatory sequences. This promotes an often substantial re-programming of the cellular proteome that enables the organism or cell to adapt to, or counteract, its changing circumstances.

Recent Advances. Significant progress has been made recently in the structural and mechanistic characterization of iron-sulfur cluster regulators and, in particular, the O_2 and NO sensor FNR, the NO sensor NsrR, and WhiB-like proteins of Actinobacteria. These are the main focus of this review.

Critical Issues. Striking examples of how the local environment controls the cluster sensitivity and reactivity are now emerging, but the basis for this is not yet fully understood for any regulatory family.

Future Directions. Characterization of iron-sulfur cluster regulators has long been hampered by a lack of high resolution structural data. Though this still presents a major future challenge, recent advances now provide a firm foundation for detailed understanding of how a signal is transduced to effect gene regulation. This requires the identification of often unstable intermediate species, which are difficult to detect and may be hard to distinguish using traditional techniques. Novel approaches will be required to solve these problems.

Keywords: iron-sulfur; DNA regulator; O_2; nitric oxide; redox stress

Introduction

Iron-sulfur proteins exhibit a remarkable breadth of structural and functional diversity. They function in electron transfer and storage, chemical catalysis, structural stabilization, and small molecule sensing (4,9,13,87). They are characterized by the presence of an iron-sulfur cluster, a protein cofactor that contains iron and inorganic sulfide. They are extremely widespread in nature and are amongst the most ancient of protein cofactors. The [2Fe-2S] cluster is the simplest, consisting of a $[Fe_2\text{-}(\mu_2\text{-}S)_2]$ rhomb, with each iron coordinated by two further ligands that are normally amino acid residue side chains, see Figure 1. This arrangement provides tetrahedral coordination at each iron. The [4Fe-4S] cluster consists of two interpenetrating tetrahedra of iron and sulfide ions, forming a cube that is linked to the protein framework by a minimum of three amino acid residues lying at the vertices of a tetrahedron (27). The loss of one iron from a vertex of a [4Fe-4S] cluster cube generates a [3Fe-4S] cluster. These are generally much less common than [2Fe-2S] and [4Fe-4S] clusters and are sometimes observed as intermediates of cluster conversion reactions, or as the result of damage to a [4Fe-4S] cluster (Figure 1) (10,26). There are other, more exotic iron-sulfur clusters found in biology, e.g. (97,149), but these are not involved in sensing functions and so will not be considered further here. Cysteine thiolates (RS^-) are by far the most commonly found amino acid ligands to cluster iron ions, but other residues such as histidine (-N=), serine ($R\text{-}O^-$) and aspartate (RCO_2^-) are occasionally found (for examples see (16,60,68,105,109,176,177)).

The capacity to participate in redox chemistry is a key functional characteristic of many iron-sulfur clusters, but this also means that they are readily damaged through interaction with redox-active species such as molecular oxygen (O_2), superoxide ions and hydrogen peroxide, leading, usually, to cluster degradation or even complete loss (70). In general the abundance of iron-sulfur clusters correlates inversely with the presence of O_2, reflecting this reactivity and fragility (66,74). Clusters are also susceptible to damage via interactions with strongly coordinating species. For example copper and cobalt disrupt iron-sulfur clusters and this is a route through which these metal ions exert toxicity (108,136). Nitric oxide (NO) also reacts with iron-sulfur clusters, forming various iron nitrosyl species. The formation of such species

requires a supply of electrons, and so, in this case, coordination reactions are coupled to redox chemistry (171).

The inherent reactivity of iron-sulfur clusters with a range of small molecules makes them ideal candidates for roles in sensing environmental change and stress caused by reactive oxygen species (ROS) and reactive nitrogen species (RNS). Moreover, because clusters of different nuclearity and shape can interconvert, they can drive protein conformational change, with significant effects on protein-DNA interactions and hence a means to effect transcriptional regulation.

Here, we review the roles of iron-sulfur cluster proteins that function in sensing redox signals, defined broadly to include O_2 and NO sensing, which both involve cluster redox chemistry. We highlight the most recent advances, with particular emphasis on new high resolution structural and mechanistic data that illustrate the complex and fascinating chemistries of these cofactors.

Primary versus secondary signals

In this review, we categorize the various known iron-sulfur cluster regulators according to the primary signal to which they respond. However, in many cases, a regulator will respond to other species in addition to their primary signal. For example, and as discussed in more detail below, SoxR and thus the SoxRS regulon in *E. coli* is activated by NO (37), but it primarily responds to redox active molecules such as methyl viologen (148). A dedicated or primary sensor can be thought of as one that directly detects its primary analyte (such as NO), or chemically related products (such as S-nitroso-glutathione (GSNO)), and modulates the expression of genes producing proteins whose actions are directly related to the primary analyte. A secondary sensor would therefore be capable of detecting other analytes besides the primary one, and modulating the expression of genes that may be considered useful when dealing with the secondary analyte. As noted by Spiro (157), determining the primary analyte can be a difficult issue, especially where limited *in vivo* or *in vitro* studies exist.

Sensors of molecular oxygen and ROS

Many bacteria exhibit remarkable metabolic flexibility that enables them to respire both in the presence and absence of O_2. While the greater efficiency of O_2 makes it the preferred terminal electron acceptor for respiration, other compounds, such as nitrate and fumarate, can be used when O_2 is limiting (169). This flexibility is dependent on the ability to sense O_2 and to make suitable adjustment of the cellular proteome. However, along with the energetic advantages of aerobic respiration comes the dangers associated with the incomplete reduction of O_2, which results in the generation of ROS, such as superoxide ion, hydrogen peroxide and the hydroxyl radical (70). Moreover, redox-cycling molecules such as the antibiotic actinorhodin are toxic, even in the absence of O_2 (61). Thus, it is essential that cells can respond to, and minimize, the toxicity associated with not only ROS, but also naturally occurring redox-active molecules.

FNR family regulators

In *E. coli,* and many other bacteria, the O_2-sensing fumarate and nitrate reduction (FNR) protein is the master regulator of the switch between aerobic and anaerobic metabolism, regulating >300 genes, over dissolved O_2 tensions in the range of 0 – 20 μM (8,62,63,88,110,170). The first crystal structure of an FNR, from *Aliivibrio fischeri*, was recently reported with its [4Fe-4S] cluster intact, see Figure 2A (176). *A. fischeri* FNR is highly homologous to *E. coli* FNR (84% sequence identity) and so the structural insight gained maps directly on to the wealth of *in vivo* and *in vitro* data available for the *E. coli* protein. Like other members of the CRP-FNR superfamily of regulators, FNR comprises two distinct domains, providing sensory and DNA-binding functions, respectively, linked by a dimer interface. The N-terminal sensory domain contains four essential Cys residues (Cys20, 23, 29 and 122) (59,85,86) that are capable of binding either a $[4Fe\text{-}4S]^{2+}$ (Figure 2B) or a $[2Fe\text{-}2S]^{2+}$ cluster. In the absence of O_2, monomeric FNR (~30 kDa) acquires a $[4Fe\text{-}4S]^{2+}$ cluster via the Iron-

sulfur cluster (Isc) biosynthetic system (115,145). This triggers a conformational change at the dimerization interface that leads to the formation of homodimers (~60 kDa) and site specific DNA binding sites within target promoters via a C-terminal helix-turn helix domain. Kiley and colleagues established early on that the presence of O_2 led to the conversion of $[4Fe\text{-}4S]^{2+}$ FNR into a $[2Fe\text{-}2S]^{2+}$ form (85,101), both *in vivo* and *in vitro*, leading to monomerization and loss of DNA-binding (84,100).

A model of the FNR monomer interface had been proposed previously based on a series of studies of site-directed variants (6,7,84,88,101,117). These studies showed that Asp154, Ile151 and Arg140, which were all predicted to lie at the dimer interface, were key residues in controlling the equilibrium (117). The recent structure of *A. fischeri* FNR shed considerable further light on the finely balanced equilibrium between monomer and dimer forms of FNR. Several aspects of the model were confirmed, but previously unrecognized aspects were uncovered. In particular, the Asp154 sidechain is located in a pocket that cannot stabilize the expected negative charge and this is most likely also an important factor alongside Asp154-Asp154 charge repulsion in destabilizing the dimer following reaction of the cluster with O_2. The sidechain of Ile151 participates in hydrophobic interactions at the coiled-coil interface that are important in stabilizing the dimer in the absence of O_2. Furthermore, Arg140 forms a salt bridge with Asp130 from the opposite monomer that also stabilizes the dimer, and disruption of this interaction is most likely a key step in destabilizing the dimer upon cluster reaction with O_2, triggering an 'unzipping' of the coiled-coil dimer interface from the top to the C-terminal end of the interfacial helices (176)

A range of biophysical techniques have been used to study the FNR cluster conversion in detail. Through a combination of visible absorbance and EPR spectroscopies, an EPR active $[3Fe\text{-}4S]^{1+}$ ($S = ½$) species was identified as a transient intermediate, indicating a two-step process (see Scheme 1) (25,26).

Scheme 1

Step 1: $[4Fe\text{-}4S]^{2+} + O_2 \rightarrow [3Fe\text{-}4S]^{1+} + Fe^{2+} + O_2^-$

Step 2: $[3Fe\text{-}4S]^{1+} \rightarrow [2Fe\text{-}2S]^{2+} + Fe^{3+} + 2S^{2-}$

In the first step, a Fe^{2+} ion is released to generate the $[3Fe\text{-}4S]^{1+}$ intermediate. This likely occurs following one electron oxidation of the $[4Fe\text{-}4S]^{2+}$ cluster to yield an unstable $[4Fe\text{-}4S]^{3+}$ cluster that ejects Fe^{2+}. The second step corresponds to the conversion of the $[3Fe\text{-}4S]^{1+}$ species to the $[2Fe\text{-}2S]^{2+}$ cluster. Cluster sulfide is either ejected into aqueous solution or undergoes oxidation to form sulfane (S^0), which can form persulfides with the thiolate side chain of Cys residues. Cys persulfides can serve as ligands to the [2Fe-2S] cluster, as recently demonstrated, see Scheme 2 (122,186). Thus, the second step may also be O_2 dependent and hence more complex than initially envisaged. Note, the $[2Fe\text{-}2S]^{2+}$ cluster of FNR is also not very stable in the presence of O_2 and slowly degrades *in vitro* and *in vivo* to give cluster-less (apo-) protein (1,139,161). Apo-protein can incorporate a 'fresh' cluster, as demonstrated *in vivo* by the reactivation of FNR in cells where protein synthesis was inhibited (36). *In vitro* cluster reconstitution reactions, which enable post-isolation insertion of a cluster, exploit this ability.

Scheme 2

Step 2: one persulfide ligand

$[3Fe\text{-}4S]^{1+} + O_2 + 2H^+ \rightarrow [2Fe\text{-}2S]^{2+}(S) + Fe^{3+} + S^{2-} + H_2O_2$

Step 2: two persulfide ligands

$[3Fe\text{-}4S]^{1+} + O_2 + 4H^+ \rightarrow [2Fe\text{-}2S]^{2+}(S)_2 + Fe^{3+} + 2H_2O$

To probe the cluster conversion reaction further, and in particular to gain insight into the [3Fe-4S] to [2Fe-2S] part of the reaction, electrospray ionization mass spectrometry (ESI-MS) was recently employed under conditions where the protein remained folded with the cluster bound. This work utilised an O_2-tolerant variant of FNR, S24F, which was previously

shown to react via the same mechanism as wild type FNR (72), but at a slower rate, thus enabling real-time mass spectrometry measurements. The data provided an unusually detailed view of the cluster conversion process through the simultaneous detection of reactants, intermediates and product species, see Figure 3A. Global analysis of the cluster conversion kinetics, as monitored by ESI-MS, was consistent with previous spectroscopic studies showing that the first step of the reaction is the loss of Fe^{2+} from the $[4Fe\text{-}4S]^{2+}$ cluster to form a $[3Fe\text{-}4S]^{1+}$ cluster intermediate (Figure 3B). Cluster-specific ^{34}S isotopic substitution was used to unambiguously assign intermediary iron-sulfur species, see Figure 3C (24-26). Once formed, the $[3Fe\text{-}4S]^{1+}$ cluster is only transiently stable. The ESI-MS data revealed the formation of a novel [3Fe-3S] cluster, which formed and decayed as a true conversion intermediate. This species results from the loss of one sulfide ion from the $[3Fe\text{-}4S]^{1+}$ cluster, implying that the product is a $[3Fe\text{-}3S]^{3+}$ species. Independent evidence for the existence of a protein bound $[3Fe\text{-}3S]^{3+}$ cluster comes from non-denaturing ESI Fourier transform ion cyclotron resonance MS studies on the [3Fe-4S] cluster of *Pyrococcus furiosus* FdI, where it appeared to result from instability of the cluster (73). An inorganic model $[3Fe\text{-}3S]^{3+}$ cluster, which has a paramagnetic, S=1/2 ground state, was recently described. We note that the X-band EPR spectrum of the model complex was similar to those of $[3Fe\text{–}4S]^{1+}$ clusters, including those recorded for S24F and wild type FNR proteins during cluster conversion (26,72,102). The decay of the [3Fe-3S] intermediate was found to be relatively slow and represents the rate limiting step of the [3Fe-4S] to [2Fe-2S] conversion process. Indeed, the observed rate constant is comparable to that previously reported for the [3Fe-4S] to [2Fe-2S] conversion of both the S24F variant and wild type FNR (72)). If the [3Fe-3S] cluster intermediate is similar in arrangement to the hexagonal planar array of three Fe^{3+} and three sulfide ions observed in the model [3Fe-3S] cluster, this would suggest a mechanism by which the cuboid [4Fe-4S] cluster may rearrange to form the planar [2Fe-2S] rhomb.

Non-denaturing ESI-MS data revealed the presence of both monomeric and dimeric FNR (33). Although the [4Fe-4S]/[4Fe-4S] FNR dimer was readily detected, only very minor amounts of dimer-associated [3Fe-4S] or [3Fe-3S] species were observed. This strongly

indicates that, as soon as a Fe^{2+} ion is lost from one $[4Fe\text{-}4S]^{2+}$ cluster (on one subunit of the dimer), the stability of the dimer is reduced and the monomer-dimer equilibrium becomes heavily favored in the direction of the monomer. We note that a dimeric form of *A. fischeri* FNR, containing a partly degraded cluster, displays a disorganized cluster binding loop (residues 20 to 29) following the loss of iron(s) (176). This suggests that Cys20 is the first residue to dissociate from the cluster. Dissociation of Cys20 would increase the flexibility of the Cys20-Cys29 cluster binding loop, which is likely an important initiating step in the conformational changes that accompany cluster conversion.

Resonance Raman and LC-MS studies had previously shown that cluster sulfide becomes oxidized to sulfane during the cluster conversion process and that it can be incorporated into the Cys-iron bonds that coordinate the [2Fe-2S] cluster, as persulfides (186). However, when sulfide oxidation occurs in relation to cluster conversion in FNR remained unexplored: is it simultaneous with the conversion process, or a subsequent reaction? Non-denaturing ESI-MS kinetic data showed clearly that sulfide oxidation occurred at the same time as formation of the [2Fe-2S] cluster, leading to [2Fe-2S] and singly and doubly persulfide coordinated species forming simultaneously. This was confirmed through time resolved LC-MS experiments carried out under identical conditions to the non-denaturing MS experiments. A summary of the mechanism of FNR cluster conversion is shown in Figure 4.

Cys persulfides can act, at least *in vitro,* as a stored form of sulfur, allowing the original cluster to be repaired on supply of electrons and Fe^{2+} (186). Thus, FNR may function by a continual process of cycling between active [4Fe-4S], inactive [2Fe-2S] and apo forms, with the level of O_2 determining which form predominates and, therefore, the extent to which FNR is transcriptionally active (see Figure 4). This type of regulatory control requires that FNR levels are tightly controlled (72), and it is known that this is the case in *E. coli* where FNR levels vary little under different growth conditions (114,160).

Bacillus subtilis FNR exhibits significant differences to the *E. coli* protein. In particular, the [4Fe-4S] cluster is located in the C-terminal domain, and, unusually, is coordinated by three Cys residues (Cys227, 230 and 235) plus an aspartate (Asp141) (60,138). Another

major difference to *E. coli* FNR is that the cluster is not required for dimerization, though it is essential for the activation of FNR-regulated genes, and, therefore, functions as a sensory unit. In contrast to *E. coli*, levels of *B. subtilis* FNR are variable depending on the O_2 concentration (up-regulated at low O_2 and down-regulated at high O_2). This, together with the major differences in the cluster binding and location, suggests that the *B. subtilis* protein may function differently from *E. coli* FNR. The regulation of anaerobic metabolism in *Bacillus subtilis* has recently been reviewed (67).

FnrP, the *Paracoccus denitrificans* orthologue of FNR, also binds a [4Fe-4S] cluster but has a different arrangement of Cys residues at its N-terminus (69). FnrP undergoes O_2 driven cluster conversion similarly to *E.coli* FNR, but at a rate approximately six fold lower (12,28). This suggests that FnrP remains transcriptionally active at higher O_2 tensions than *E. coli* FNR, consistent with a role for FnrP in activating expression of the high O_2 affinity cytochrome *c* oxidase (*cco*) in *P. denitrificans* under microaerobic conditions (126).

The role of FNR as a master regulator of the anaerobic to aerobic switch means that it is likely to be important for virulence of pathogens that encounter fluctuations in O_2 concentration as they seek to establish infection. In *Salmonella enterica* serovar Typhimurium, FNR was shown to be essential for infection in a mouse model and for survival in the macrophage (47), and this was associated with the inability of an *fnr* mutant to respond to the cytotoxic oxidative burst associated with the NADPH phagocyte oxidase. Similar observations have been made for *Neisseria meningitidis* and *Laribacter hongkongensis* (5,40,183). The type III secretion system critical to *Shigella flexneri* virulence is controlled by FNR-mediated regulation of Ipa secretion (111). This regulation ensures that type III secretion is functional only at its precise site of action, i.e. in the partially oxygenated environment in the vicinity of the gastrointestinal mucosa. Recently, RNA-seq studies have shown that the influence of FNR on this process is more extensive than previously appreciated (174).

NreB

Staphylococcus lacks an FNR-like O_2 sensor. Instead, these bacteria employ the nitrate regulatory element (Nre), a multi-component system encoded by the *nreABC* operon, which regulates the expression of genes associated with anaerobic nitrate/nitrite respiration (45). NreB and NreC together constitute a two-component regulator: NreB is a cytoplasmic sensor kinase and NreC is a response regulator. NreB has a PAS domain at its N-terminus with four Cys residues (Cys59, 62, 74 and 77) and can bind a $[4Fe\text{-}4S]^{2+}$ cluster (80,119). In the presence of O_2, the cluster undergoes conversion to a [2Fe-2S] form, and subsequently to the apo-form. NreB functions as a cytoplasmic histidine kinase, and is dependent on the presence of the [4Fe-4S] cluster. Thus, like FNR, NreB is a direct O_2 sensor, but, unlike FNR, it does not itself act as a transcriptional regulator (80). Instead, through its kinase activity, NreB activates NreC, which in its phosphorylated form can bind to specific sequences upstream of anaerobic respiratory *nar* and *nir* operons (45,80).

NreA has recently been shown to constitute a new type of nitrate receptor. The structure of NreA with bound nitrate was solved at 2.35 Å resolution, revealing a GAF domain fold (123). How NreA functions was recently clarified through studies of the *Staphylococcus carnosus* Nre system. In the absence of nitrate, NreA inhibits Nre-mediated activation through interaction with NreB (123). The introduction of nitrate leads to binding to NreA, which must cause a conformational change that reduces the extent of interaction between NreA and NreB, alleviating the inhibitory effect on NreB. The current understanding of the NreABC system is summarized in Figure 5.

SoxR

Bacteria are exposed to a multitude of redox active molecules that may serve as quorum signals, virulence factors or antibiotics. Many of these compounds are produced to help bacteria commandeer resources and/or gain an edge over competing species, while others are man-made. The herbicide methyl viologen (Paraquat) is an example of the latter; it can abstract an electron from NAD(P)H-reduced flavin cofactors, which can rapidly react with O_2,

regenerating the oxidized form along with reactive oxygen species (ROS) such as $O_2^{-\cdot}$ and/or H_2O_2 (19). If allowed to proceed in an uncontrolled manner, this redox cycle is fatal.

The SoxRS system constitutes an unusual two-part regulatory system in enteric bacteria, in which the two proteins act sequentially to activate transcription of >100 genes in response to redox active molecules or ROS. SoxR, which belongs to the MerR family of metal-responsive transcriptional regulators, exists as a homodimer in solution, containing one [2Fe-2S] per monomer, coordinated by residues Cys119, 122, 124 and 130. Although the cluster is not required for structural stability or DNA binding, it is essential for *in vivo* activation of *soxS* transcription, the only well-established target for SoxR. The SoxS protein, also a transcriptional activator, switches on the expression of a suite of genes, including a Mn-superoxide dismutase, multi drug efflux systems and antibiotic resistance like transcriptional regulators. It also adjusts metabolism to favor NAD(P)H regeneration. SoxS is also subject to rapid proteolytic degradation, thus ensuring the two-component system response remains highly dependent on the input signal sensed by SoxR (15,82,130,153).

X-ray structures of [2Fe-2S] SoxR in the free form and in complex with *soxS* promoter DNA are available, see Figure 6A. The overall architecture of SoxR is similar to other MerR family members, although significant differences exist in the alignment of the dimerization helix with the DNA-binding domain. Unusually, the [2Fe-2S] cluster is solvent exposed, held in an asymmetric electrostatic environment with the rhomb plane of the cluster tilted ~20° relative to the plane of coordinating Cys residues (181).

The [2Fe-2S] cluster can exist in +1 and +2 states, connected by a reduction potential of -285 mV (versus SHE at pH 7.6). Indeed, SoxR is readily isolated with a $[2Fe\text{-}2S]^{+}$ cluster, and is actively maintained in the reduced state, *in vivo*, at the expense of NAD(P)H (55,61,93,94,150). Only when the cluster is in the $[2Fe\text{-}2S]^{2+}$ form can SoxR activate *soxS* transcription by remodeling of the -35 and -10 promoter elements, such that they become optimally positioned for interaction with RNA polymerase. We note that the solvent exposed nature of the [2Fe-2S] cluster likely enables rapid electron transfer to and from the cluster. Indeed, it would appear that oxidation of the $[2Fe\text{-}2S]^{1+}$ cluster of SoxR can be catalyzed

directly by redox-cycling molecules, such as methyl viologen. Whether DNA-binding has an important effect on the redox properties of the cluster is unclear. Electrochemical measurements on DNA-modified electrodes revealed a dramatic increase in the reduction potential of the cluster to +200 mV for SoxR bound to its cognate DNA (58). More recent solution studies indicated a much smaller increase (~+30 mV) in potential on DNA-binding (89). Furthermore, how the cluster redox change translates into the conformational changes required to activate transcription is uncertain. The asymmetric electrostatic environment surrounding the cluster may be important. It is suggested that in the reduced +1 state the additional negative charge attracts the main chain amides towards the sulfur atoms of the cluster and repels close lying oxygen atoms. Oxidation of the cluster to the +2 state increases attraction to negatively charged carbonyl oxygen atoms. These subtle changes to the cluster binding domain lead to substantial change in the relative position of the DNA-binding domains, widening the distance between the recognition helices to accommodate the unusually long, 19bp, spacer between the -35 and -10 elements of the *soxS* promoter (181).

Although SoxR is widely distributed among bacteria, SoxS is absent in non-enteric species, such as *Streptomyces coelicolor* (148). We note that *S. coelicolor* SoxR has a higher reduction potential (~-185 mV) (153) than *E. coli* SoxR. This results in the detection of a slightly narrower range of redox active molecules in comparison to *E. coli* SoxR, and increased sensitivity to extracellular actinorhodin, an antibiotic naturally synthesized by *S. coelicolor* (148). The current understanding of the SoxRS system is summarized in Figure 6B.

RsrR

Members of the Rrf2 superfamily of transcription factors are widespread in bacteria but their functions are largely unexplored (57). The few that have been characterized in detail sense cysteine availability (CymR), nitric oxide (NsrR), the iron-sulfur cluster status of the cell (IscR) and iron limitation (RirA); several of these are discussed in detail below.

S. venezuelae RsrR (redox sensitive response regulator) was predicted on the basis of sequence to be a homologue of *S. coelicolor* NsrR (discussed below). ChIP-seq analysis

revealed that rather than regulating the nitrosative stress response, RsrR binds to a different and much larger set of genes with a diverse range of functions (120). These include a number of transcriptional regulators, genes required for glutamine synthesis, NADH/NAD(P)H metabolism, as well as general DNA/RNA and amino acid/protein turn over. Biochemical experiments showed that the protein contains a $[2Fe\text{-}2S]^{+1}$ cluster as isolated, and that it can exist in +1 and +2 states. Intriguingly, the switch between oxidized and reduced cluster controls the DNA binding activity of RsrR, with significant DNA-binding observed only when the cluster is oxidized. To our knowledge, both the sensing domain and the putative target genes are novel for an Rrf2 protein, suggesting that RsrR represents a new member of the Rrf2 superfamily, which is functionally reminiscent of SoxR (120).

Sensors of nitric oxide

The biological functions of NO are inexorably linked to its chemical properties. NO is a reactive, lipophilic radical that can freely diffuse into cells. It readily reacts with thiols, O_2^- and O_2 (amongst others), resulting in a range of species, including S-nitrosothiols, nitrogen dioxide (NO_2), peroxynitrite ($ONOO^-$), dinitrogen trioxide (N_2O_3) and nitrite (NO_2^-), whose cytotoxic chemistries are often regarded collectively as nitrosative stress. Metal (principally iron) containing cofactors are also a direct target for NO (166). Thus, proteins containing iron-sulfur clusters are highly susceptible to damage under conditions of nitrosative stress.

In higher eukaryotes, NO fulfils a wide range of biological roles, functioning as a key secondary messenger in vasodilation, a neurotransmitter, and as a cytotoxin generated by the immune system as the first line of defence against pathogen invasion (182). Thus, many pathogenic bacteria have evolved a suite of specific proteins to sense NO (some of which are discussed in detail below) to enable them to counter the deleterious effects of high concentrations (> 10 μM) of NO generated by the host organism (76).

Such proteins are also widespread in non-pathogenic bacteria, particularly those that carry out anaerobic respiration with nitrate/nitrite as a terminal electron acceptor. Here, the

adventitious reduction of nitrite (NO_2^-) by nitrate (NO_3^-) reductases is a significant source of endogenous NO (131,175). *In vivo*, many transcriptional regulators respond to the presence of aqueous NO, acidified nitrite or S-nitroso-glutathione; in *E. coli* these include MetR, IscR, Fur, FNR, SoxR, OxyR, NorR and NsrR. This can lead to a dramatic metabolic reorganization in order to adapt to stress conditions (46,48,99,132,146). In some cases, NO exposure may protect bacteria from antibiotics (e.g. aminoglycosides) by disrupting the energy-dependent uptake of these drugs, while NO is a natural intermediate in the conversion of NO_3^- to N_2 for denitrifying bacteria (64,65,112,167).

Many literature reports of reactions of NO with protein-bound iron-sulfur clusters ([2Fe-2S], [3Fe-4S] or [4Fe-4S]) have identified the product as a dinitrosyl iron complex ($[Fe(NO)_2](RS)_2$, DNIC, see Figure 7). This species has invariably been detected, both *in vivo* and *in vitro,* by means of its distinctive S = ½ EPR signal, at g = 2.03. However, when quantified by spin integration, the amount of DNIC accounts for only a few percent of the iron in the original cluster (see (30) and references therein). Examination of the inorganic chemistry of DNIC complexes reveals that they exist in equilibrium with an EPR silent Roussin's Red Ester ($[Fe_2(NO)_4](RS)_2$, RRE) type species in a thiol dependent manner (21,172). We note that higher nuclearity iron-nitrosyl species are also possible (reviewed by (104)), with the most common of these being Roussin's Black Salt ($[Fe_4S_3(NO)_7]$, RBS), see Figure 7.

Wbl proteins

The WhiB-like (Wbl) family of regulators are named after white (*whi*) *Streptomyces coelicolor* mutants that are arrested at different developmental stages of sporulation and fail to produce the usual grey spore pigment (34). They are confined to Actinobacteria, a phylum of Gram-positive bacteria that includes *Streptomyces*, *Bifidobacterium,* as well as important human pathogens such as *Mycobacterium tuberculosis* and *Corynebcterium diphtheria* (156). Many Actinobacteria contain multiple Wbl proteins, which are generally small (~9 – 15 kDa) and consist of a variable N-terminal region and a core region that contains a highly-conserved pattern of Cys residues (Cys-X_n-Cys-X_2-Cys-X_5-Cys) that, in all cases reported to date, binds

an iron-sulfur cluster. The C-terminal region contains a unique turn motif (GVWGG), followed by a putative DNA binding region rich in positively charged residues that is annotated as a AT-hook motif in some cases (35,133,135,154). Despite this, the function of Wbl proteins has been the subject of some controversy, in part because of the lack of evidence of 'traditional' DNA-binding behavior. Cluster-free Wbl proteins have been proposed to function as protein disulfide reductases, becoming activated through cluster loss (caused by, e.g., oxidative stress) (2,53,54,92). However, the majority of more recent evidence now indicates that Wbl protein are indeed DNA regulatory proteins that utilize their iron-sulfur cluster as a sensory unit to directly or indirectly modulate DNA-binding (20,22,23,43,135,141,151,155).

In *M. tuberculosis*, Wbl proteins function in the pathogen's remarkable ability to persist within its host, as well as its innate resistance to a wide range of antibiotics. From a physiological perspective, *M. tuberculosis* WhiB3 is perhaps the best understood of all the Wbl proteins. *In vivo*, *whiB3* expression is upregulated in response to NO and an acidic extracellular pH, and [4Fe-4S] WhiB3 is sensitive to NO, with exposure enhancing site specific DNA binding (151). This results in production of storage lipids (principally triacylglycerol) and virulence determinants (e.g. polyketides) (143,151,152), with the latter disrupting phagosomal maturation and acidification (113,143). WhiB3 also regulates the production of ergothioneine (142), a low molecular weight thioketone that is critical for the survival of *M. tuberculosis* inside macrophage phagosomes (140).

[4Fe-4S] WhiB6 from *M. marinum* (closely related to *M. tuberculosis*) differentially regulates dormancy (DosR) and the virulence (ESX-1) regulons through its ability to sense NO and oxidative stress (23). WhiB6, via ESX-1, regulates the export of virulence factors that enable the bacterium to survive in the macrophage by escaping the phagosome. Sustained exposure to exogenous ROS and RNS from the host's immune system leads to apo- and nitrsoylated forms of WhiB6, which promote a shift away from aerobic respiration and into dormancy, via the DosR/S/T system, enabling *M. marinum* to establish a persistent infection within the granulomas. WhiB7, which regulates aspects of innate resistance to a variety of

therapeutic antibiotics (17,135), along with WhiB3 has been shown to interact with the principal sigma factor SigA (17,18,158).

Streptomyces coelicolor encodes 11 Wbl proteins of which five, WblE (WhiB1 in *M. tuberculosis*), WhiB (WhiB2), WhiD (WhiB3), WblA (WhiB4) and WblC (WhiB7), are well conserved in other Actinobacteria species. As for *M. tuberculosis*, many of these proteins function in cell developmental processes (sporulation) and in antibiotic resistance (71,116,118). Recently it was shown that WblC (WhiB7) induces a stable isoform of the ECF sigma (σ) factor R that governs the thiol-oxidative stress response, and that WblC binding to the sigRp1 promoter responds to antibiotic treatment *in vivo* (184). Furthermore, WhiB was recently shown to function in concert with WhiA to control genes required for initiation of sporulation and septation (20). WhiA is an unusual transcription factor that consists of a homing endonuclease fused to a "domain 4" of a bacterial sigma 70 protein (77,78). Substitution of the cluster coordinating Cys residues in WhiB was sufficient to prevent DNA binding by both WhiA and/or WhiB *in vivo,* consistent with them working in concert (20). The interaction of Wbl proteins with protein partners (often sigma factors or sigma factor-like proteins) may represent an important aspect of their biological mechanism and functional diversity.

The *in vitro* reactions of *M. tuberculosis* WhiB1 and *S. coelicolor* WhiD with NO have been examined in detail using spectroscopic and/or rapid reaction kinetic methods (30,155). These studies revealed a rapid multi-NO (~8 per cluster), multi-phasic reaction that appears to be characteristic of [4Fe-4S] cluster containing regulators. The first step of the reaction was found to be first order with respect to NO with an apparent second-order rate constant of k = ~6 x 10^5 M^{-1} s^{-1}. All subsequent steps were also first order in NO (30), consistent with the stepwise binding/reaction of NO. Overall, WhiD was found to be more sensitive than FNR (which has a secondary role in NO sensing, see below) but less sensitive than the primary NO sensor NsrR (see below) (30,32). These observations are consistent with WhiB1 and WhiD (WhiB3 in *M. tuberculosis*) playing a role in sensing NO, rather than ROS stress, as the rate of reaction with NO is ~10^4-fold faster than the reaction of these clusters with O_2 (30,98).

Recent studies of WhiD (and NsrR; discussed in detail below) using nuclear resonance vibrational spectroscopy (NRVS) showed that reaction with NO generated multiple iron-nitrosyl species, principally of the RRE- and RBS-types (Figure 7) (146).

Such studies of [4Fe-4S] Wbl reactivities, together with the *in vivo* data summarized above, indicate that NO is a physiological signal for at least some Wbl proteins. Furthermore, the iron-sulfur cluster plays a key functional role in controlling DNA/partner protein-binding.

NsrR

NsrR, like RsrR described above, belongs to the Rrf2 superfamily of transcriptional regulators (29,185). It functions as a global regulator of the response to NO induced stress in many bacterial species, and is important for virulence (*S. enterica)* or host colonization (*A. fischeri*) (38,56,81,90,127,180). While some Rrf2 family regulators do not contain an iron-sulfur cluster (e.g. CymR (147,164)), others, including NsrR, contain three conserved Cys residues that are known to coordinate a cluster (29,32). Many others are predicted to bind a cluster because they contain the three conserved Cys residues (e.g. RirA (165)), but the cluster type is uncertain because examples of both [2Fe-2S] (e.g. the iron-sulfur cluster biogenesis regulator IscR (134) and RsrR) and [4Fe-4S] (NsrR) are known. Which cluster is utilized presumably depends on the particular role of the regulator and the signal it senses, but this is not currently well understood.

In both, *E. coli* and *B. subtilis,* NsrR proteins have been shown to regulate multiple genes, including the NO detoxifying flavohaemoglobin, *hmp* (46,90). *B. subtilis* NsrR is somewhat unusual amongst NsrR proteins (but similar to IscR (121)) in that it can bind two different types of operator sites. These are termed class I / class II, and only binding to class I is dependent on the cluster (90,91). Recent ChIP-seq experiments indicated that *S. coelicolor* NsrR controls only three genes: *hmpA1, hmpA2* (both encoding NO detoxifying flavohaemoglobins) and *nsrR* itself. Thus, *S. coelicolor* NsrR appears to have a specialized regulatory function, controlling an operon focussed solely on NO detoxification, it is, therefore not a global transcriptional regulator (29).

NsrR purified under anaerobic conditions is a dimer containing one [4Fe-4S]$^{2+}$ cluster per monomer (29,185). Through a combination of electrophoretic mobility shift assays (EMSA) and DNaseI foot-printing, *S. coelicolor* [4Fe-4S] NsrR was shown to bind site specifically and tightly to an 11bp inverted repeat sequence within the promoter regions of the identified target genes, with binding tightest to the *hmpA1* promoter (saturation was observed at a ratio of [4Fe-4S] NsrR monomer to DNA of approximately 2:1, i.e. one NsrR dimer per DNA) (29). Binding to *hmp2A* and *nsrR* promoters was weaker, with full binding occurring at ratios of ~8 and ~5, respectively. Unlike *B. subtilus* NsrR, apo-NsrR had no affinity for any of these promoters (29).

A range of biophysical techniques have been used to study NsrR in detail. It was found that some low molecular weight thiols (such as DTT) could modify the [4Fe-4S] cluster (29,185), and for *S. coelicolor* NsrR this was shown to drastically reduce its O_2 stability, leading to rapid disassembly into a [2Fe-2S] cluster. These observations help account for initial reports of a [2Fe-2S] form of *S. coelicolor* NsrR (168). Importantly, physiological thiols, such as cysteine or mycothiol, did not induce cluster conversion (29). Resonance Raman data collected from [4Fe-4S] NsrR samples were consistent with an iron-sulfur cluster coordinated by three Cys and one oxygen-containing residue, rather than a histidine residue as found in IscR (29,49). Thus, where exogenous thiol binding is observed, this is most likely due to competition for the unique iron site that is not coordinated by a cysteine residue (29,185).

Very recently, the 1.95 Å resolution crystal structure of *S. coelicolor* [4Fe-4S] NsrR was reported, the first Rrf2 family regulator structure with a cluster bound, see Figure 8A (177). Like other Rrf2 members, NsrR is a homo-dimer, with each monomer consisting of a DNA-binding domain (a winged helix-turn-helix motif) together with an elongated dimerization domain. The [4Fe-4S] cluster is ligated, as expected, by the three conserved Cys residues (Cys 93, 99 and 105), which form a distinct loop. Unexpectedly, the fourth ligand is provided by Asp8 from the opposite monomer(Figure 8B). NsrR appears to represent the first structurally characterised example of an asymmetrically bound [4Fe-4S] cluster, were ligands are provided from two different subunits. To evaluate the importance of the carboxylate ligand,

D8C and D8A variants were generated. These both retained the ability to bind a [4Fe-4S] cluster but DNA-binding affinity was either reduced or abolished (177).

The cluster environment is mainly hydrophobic, without H bonds to the sulfides of the cluster. Cys93 is the only solvent exposed residue, while Cys99 and 105 are more buried and additionally stabilized through H bonds between their thiolates and the main chain N atoms of Leu101 and Arg108, respectively. Cys105 is also stabilized by a positive dipole moment from the dimerization helix. Asp8, located on the ancillary helix of the helix-turn-helix (HTH) motif, forms a salt bridge with Arg12 from the same helix, and the latter also interacts with the carbonyl oxygen atom of Val36, located within the HTH motif. An inter-subunit H bond between Gly37 and Asn97 provides additional contact between the HTH motif and the cluster binding loop.

Initial attempts to identify the fourth, oxygenic ligand of the cluster, based on cluster and DNA-binding characteristics, pointed to Glu85 as a possible ligand (29). Although now obviously not a ligand, the structure shows that Glu85 provides additional contacts with the ancillary helix, forming H bonds with the main chain N of Thr4 and the O of Thr7. In an E85A variant, these interactions would be disrupted rendering the DNA binding domain, including Asp8, more flexible (Figure 9A), accounting for the observed effects of the substitution on cluster and DNA-binding.

To gain further insight into the role of the [4Fe-4S] cluster in DNA binding, the structure of apo-NsrR (generated as a triple Cys→Ala variant) was also solved (177). In the absence of the cluster, the salt bridge between Asp8 and Arg12 remains intact, but the Arg12-Val36, Gly37-Asn97 and Glu85-Thr4/Thr7 H bonds are all disrupted. Other notable changes include the N-terminal lengthening of the dimerization helix to include Cys105, and a considerable C-terminal lengthening of helix 5 to include Cys93 (Figure 9B). The different orientations of the main chains between the holo- and apo- forms result in an opening of the iron-sulfur cluster binding domains and displacement of the recognition helix; it is likely that this is sufficient to prevent DNA binding (177).

Upon exposure to increasing concentrations of NO, NsrR eventually loses its ability to bind to DNA. Binding of [4Fe-4S] NsrR to the *hmpA2* promoter was reduced by 50% at a ratio of ~1.4 [NO]:[4Fe-4S], and lost entirely by a ratio of ~2.5. For *hmpA1* equivalent ratios were ~2.3 (50%) and ~4.2 (complete loss), while for the *nsrR* promoter ratios were ~4.1 (50%) and 8.2 (complete loss). These results suggest that *hmpA2* may be preferentially activated at low concentrations of NO. Together these observations demonstrate an interesting, but poorly understood, effect, which is presumably governed by the specific promoter sequence (32).

The sequential addition of sub-stoichiometric amounts of NO allowed changes in the absorbance of the cluster to be observed during the nitrosylation reaction. The final spectrum had an absorption maximum at 360 nm and a shoulder at ~430 nm, consistent with the formation of iron-nitrosyl species similar to RRE and RBS-type species. A plot of absorbance changes versus the ratio of NO to cluster showed that the reaction was complete at a stoichiometry of ~8 – 10 NO molecules, with a clear break point at ~2 NO molecules per cluster, and a less distinct break point at ~6 NO molecules. EPR spectra showed a DNIC signal that accounted for ~16% of total iron, the remainder being EPR silent (32).

Circular dichroism (CD) spectroscopy is particularly useful for resolving the overlapping transitions of the broad iron-sulfur cluster absorption spectrum, allowing the local cluster environment to be probed. Plots of CD intensity as a function of NO were essentially complete by ~ 8 NO, as for absorbance measurements. However, they clearly demonstrated the formation of an intermediate at 2 NO (with an intense CD band at (+)330 nm), which subsequently reacted with further NO to give less distinct intermediates at ~4 and ~6 NO. Similar CD experiments in the presence of a 23bp oligonucleotide containing the *hmp1A* promoter revealed that the major features (at ~2 and ~6 NO) of the NO response were the same as in the absence of DNA. Taken together, the titrations suggest a series of intermediates are formed during cluster nitrosylation (32). However, the nature of these intermediate species could not be determined from these data.

Recently, NRVS, utilising $^{32}S/^{34}S$ and $^{14}NO/^{15}NO$ isotopic substitutions, together with density functional theory (DFT) calculations, was used to probe experimental and theoretical

responses of [4Fe-4S] NsrR to NO. It was demonstrated that the nitrosylation reaction does not result in a single, iron-nitrosyl product, but rather a mixture of products containing principally RRE- and RBS-type species, together with smaller amounts of EPR active DNIC (Figure 7). Importantly, the $^{32}S/^{34}S$ isotope shift data from samples specifically labeled at the cluster sulfides, together with DFT calculations, showed that the RBS-type species cannot be RBS itself because $^{32}S/^{34}S$ shifts in the iron-sulfur region of the NRVS were not observed, ruling out a primarily sulfide-bridged species such as RBS. DFT calculations indicated than RBS-like species (that could be described as a Roussin's black ester, RBE, Figure 7), in which one or more of the sulfide bridges present in RBS are replaced by Cys thiolate bridges, could account for the observed spectra. Such species were predicted to have an NRVS spectrum similar to RBS, but importantly with little or no shift due to the $^{32}S/^{34}S$ isotope substitution (146).

Rapid reaction kinetic experiments (performed with data acquisition at 360 nm and 420 nm) revealed a rapid, complex multi-phased reaction that was modeled most simply as a five-step reaction. The rate of the first step was first order with respect to NO concentration (as were all subsequent steps) and most likely corresponds to binding of the first NO to the [4Fe-4S] cluster (32). Its associated second order rate constant was $k = 4.5 \times 10^6\ M^{-1}\ s^{-1}$, ten-fold higher than that for any other regulator characterised thus far by similar methods. At higher concentrations of NO (≥20 [NO]:[FeS]) the rate for the initial step became independent of NO (k = ~600 s^{-1}), indicative of a rate limiting step which does not involve NO. This is likely to correspond to the dissociation of a cluster ligand(s) and associated conformational changes that must occur before NO can bind. At low ratios only the early phases of the reaction were observed. This is consistent with there being sufficient NO to achieve the formation of only the earliest intermediate(s). Hence, the second step may represent the binding of a second NO to form an intermediate with clear spectroscopic characteristics, and an ability to modulate DNA binding (in the case of *hmpA2*)(32). This now requires further investigation.

Cavity maps (probe radius of 0.6 Å) generated from the [4Fe-4S] NsrR crystal structure of NsrR point to Asp8 as the initial point of NO binding. It is likely that this pathway is also accessible to exogenous DTT and CN^-, accounting for how these ligands are able to react with

the cluster, most likely by displacing Asp8 (29,185). As already noted above, Asp8 is intimately connected to the both the HTH motif and the cluster binding domain, and loss of its interaction (e.g. in D8A) is sufficient to cause a loss of DNA binding. Moreover, we note that in certain ferredoxins, where a [4Fe-4S] cluster is ligated by three Cys and an Asp residue, the carboxylate bound iron is readily lost, consistent with this ligand having greater lability than the Cys residues (177).

To date, the structural and biophysical data collected for *S. coelicolor* NsrR provide the most complete picture of the enigmatic nitrosylation process, but further investigations are needed to try and establish the precise nature of the nitrosylation intermediates and their physiological significance. Overall, data on *S. coelicolor* NsrR are consistent with the idea that NsrR acts as a primary NO sensor, coordinating the expression of *hmpA1/2* as the first line of defense against NO (29,32,177) (see Figure 9C). Kinetic analyses of NsrR and WhiD from the same organism suggest that NO would preferentially react with NsrR in the *S. coelicolor* cytoplasm, consistent with the idea of a hierarchy of transcriptional response. However, caution is required because there are other components of the *S. coelicolor* cytoplasm that are capable of sensing NO (e.g. DevSR)(29,32,144).

Detection of NO by FNR and SoxR

Under anaerobic conditions, nitrogen oxides, such as nitrate or nitrite, can be utilized as terminal electron acceptors in place of O_2. In this respect, we note that NarG represents the most important source of endogenously derived NO during nitrate/nitrate respiration (175). Anaerobic exposure of *E. coli* to physiologically relevant concentrations of NO led to up-regulation of multiple FNR-repressed genes (including *hmp*) and down regulation of FNR-activated genes (including *narG*), suggesting that NO inactivates FNR *in vivo* (95,132). More recently, *in vivo* transcription studies, using a semisynthetic FNR-dependent promoter, revealed a ~4 fold decrease in FNR-dependent transcription during the first 15 min following NO exposure. A more rapid response (~3 fold decrease during the first 5 min) was observed when cultures were supplemented with nitrite, a source of endogenous NO (31). The

response of FNR-dependent transcription to both exogenous and endogenous sources of NO was ~4 fold lower compared to that observed for O_2. This suggests that FNR is partially protected in the cytoplasm, most likely by the actions of the primary NO response systems. Thus, FNR is classified as a primary sensor of O_2 (or the lack thereof) that plays a secondary role in the response to NO.

In vitro studies revealed that a rapid, multi-step reaction involving ~8 NO molecules per cluster occurred upon addition of NO to [4Fe-4S] FNR, similar to the nitrosylation reactions described above for WhiD and NsrR (31). The apparent second order rate constant for the first step, which again most likely corresponds to the binding of the first NO to the cluster, was found to be $k = 2.8 \times 10^5$ M^{-1} s^{-1} (lower than for NsrR), and was first order with respect to NO at all concentrations (up to ~1 mM). The reaction resulted in monomerization of the protein, suggesting that DNA binding is abolished following NO exposure (31).

There is also increasing evidence to suggest that FnrP of *P. denitrificans* responds to NO *in vivo*, along with NsrR and NnrR (which does not contain an iron-sulfur cluster) (12,103,126). FnrP co-regulates the expression of nitrate (*nar*) and nitrous oxide (*nos*) reductases, ensuring their production under semi-aerobic conditions. *In vitro* studies of the reaction of FnrP with NO revealed significant similarities with the FNR nitrosylation reaction and also resulted in dissociation of the FnrP dimer into monomers (28).

Like FNR, it has been known for some time that SoxR-dependent activation of *soxS* can also be stimulated by NO *in vivo* (37,125). This was recently reexamined, *in vivo*, by Singh *et al*. They found that *E. coli* SoxR was activated by all of the NO-generating compounds (SNP, DETA-NO and GSNO) tested, but somewhat surprisingly, *S. coelicolor* SoxR was unresponsive (153), further reflecting the different characteristics of SoxR proteins from enteric and non-enteric bacteria. The expression of *soxS* is induced by macrophages and the SoxRS regulon appears to prolong the survival of *E. coli* in response to activated macrophages (125). This is modulated by iNOS inhibitors, suggesting that NO activation of SoxR is of physiological significance. However, microarray studies have revealed that the activity of a wide range of regulators (including both primary NO sensors such as NsrR and NorR and

secondary NO sensors such as Fur and FNR) are modulated by the presence NO (124,125,132). For some bacteria, such as *Salmonella enterica*, *soxS* is dispensable for virulence/infection and the SoxRS regulon is not significantly utilized in the presence of activated marcophages (41,44).

Exposure of [2Fe-2S] SoxR to NO leads to DNIC formation (37,106,107). The kinetics of this reaction were recently investigated using pulse radiolysis of nitrite solutions to generate NO. The reaction was found to be extremely rapid and biphasic in character. The faster phase, which corresponds to the bimolecular reaction of NO with [2Fe-2S] cluster, was reported to have a second order rate constant of k = 1.3 x 10^8 M^{-1} s^{-1}, close to diffusion controlled and approximately two orders of magnitude faster than the reaction of NO with *S. coelicolor* NsrR (32,51). Surprisingly, this implies that NO can bind without the dissociation of one of the coordinating Cys residues. Further investigations are required to verify the kinetics and intermediates of the SoxR NO reaction.

Iron regulator protein 1 and other aconitases

Aconitase, an enzyme of the citric acid cycle, is localized to the mitochondrion of eukaryotes where it functions as a dehydratase in converting citrate to isocitrate. Key to its activity is a [4Fe-4S] cluster that is coordinated by only three Cys residues, such that one iron has a vacant coordination site for substrate binding (10). Thus, the [4Fe-4S] cluster is susceptible to losing that iron, generating an enzymatically inactive [3Fe-4S] cluster that can degrade further to the apo-protein. A close homologue of aconitase is found in the cytoplasm of mammals and is known as cytoplasmic aconitase (c-aconitase) or iron regulatory protein 1 (IRP1), in recognition of its role as a key regulator of cellular iron levels.

Under conditions of iron deficiency, IRP1 loses its cluster. In its apo-form, it functions alongside IRP2 (which is not an iron-sulfur cluster protein, but is regulated in an iron-dependent manner via ubiquitin-mediated degradation (187)) to post-transcriptionally regulate the expression of genes involved in iron metabolism. It does this by binding to iron regulatory elements (IREs) at either the 5’ or 3’ ends of the mRNA transcripts, leading to either inhibition

(e.g. ferritin) or promotion (e.g. transferrin receptor) of translation (reviewed in (137,178)). High resolution structures of IRP1 in both cluster-bound and RNA-bound (as apo-protein) forms have been reported (39,179).

In addition to functioning as a sensor of iron levels, IRP1 has a specific role in responding to nitrosative stress *in vivo*. Early studies showed that NO generated in the activated macrophage/target cell system led to an increase in IRP1 IRE-binding activity in adjacent cells (14). This is consistent with the susceptibility of the IRP1 cluster to nitrosylation, resulting in protein bound DNIC complexes (83), and, therefore, sensing of NO directly by the IRP1 cluster. Studies of rat hepatoma cells showed that NO specifically increases the mRNA-binding activity of IRP1 but not IRP2 (129), consistent with more recent studies showing that IRP1 is principally responsible for the post transcriptional regulation of ferritin, ferroportin, and transferrin receptor in response to NO (159). Activation of IRP1 by NO resulted in increased iron uptake and reduced iron storage, thereby maintaining supplies of iron necessary for iron-sulfur cluster biosynthesis. Precisely how IRP1 connects and integrates the regulation of iron homeostasis and nitrosative stress *in vivo* remains unclear.

Two types of bacterial aconitase have been identified in *E.coli*; one (AcnA) is similar to the eukaryotic mitochondrial enzyme and is expressed as part of the SoxRS regulon under stress conditions. The other, AcnB, contains an additional N-terminal domain and a different domain arrangement and is therefore unique to bacteria. AcnB serves as the principal citric acid cycle enzyme but is less stable than AcnA to oxidative stress (163,173). Both AcnA and AcnB have been shown to bind to specific sequences in the 3' untranslated regions of *acnA* and *acnB* mRNA in their cluster-free forms, thereby promoting the production of the aconitase proteins under conditions of stress (eg iron starvation, or oxidative/nitrosative stress) that depletes the enzymatically active cluster-bound form (11,75,162). Intriguingly, AcnA enhances the stability of *sodA* mRNA transcripts, whereas AcnB lowers *sodA* transcript stability (82,162). Thus, the actonitase proteins of *E.coli* appear to function in a protective capacity against oxidative stress during aerobic growth (163).

Concluding remarks

Iron-sulfur cluster proteins exhibit a remarkable structural and functional diversity. Those that function as regulators of redox (oxidative, nitrosative) stress house their iron-sulfur cluster within a protein scaffold that tunes the cluster reactivity and specificity. The variety of protein folds found amongst iron-regulatory proteins, and the variety of signals that are sensed, further illustrate the diversity of these proteins. In all known cases, the cluster functions as the sensory module, and so characterization of the cluster environment and the chemistry taking place at the cluster, which includes redox cycling, cluster oxidation/degradation/conversion, and cluster nitrosylation, are critical to understanding the mechanisms that drive the conformational changes that modulate DNA (or RNA) binding. Typically, high resolution structural and mechanistic information for iron-sulfur cluster regulatory proteins is not abundant, largely owing to the sensitivity/fragility of the cluster, which has severely hampered studies of these often highly O_2-sensitive proteins. Thus, the progress made recently in solving high resolution structures of FNR and NsrR in cluster-bound states (176,177) marks a significant step forward for the field. Alongside these, *in vivo* functional studies and *in vitro* mechanistic studies have begun to establish precisely the roles that iron-sulfur cluster proteins play in cellular regulation and how they accomplish them. Future progress will require further structural characterization, particularly of DNA-bound states (such as those that are available for SoxR (181) and IscR (134)), and the development and application of new methods that can provide information on the intermediate species formed during sensing at iron-sulfur clusters. The applications of NRVS (146) and ESI-MS (33), discussed here, indicate that such methods are now becoming available.

Acknowledgments

Our work on iron-sulfur regulatory proteins has been generously supported by the UK's Biotechnology and Biological Sciences Research Council, most recently through grants BB/J003247/1, BB/L007673/1 and BB/K02115X/1.

Author Disclosure Statement

No competing financial interests exist.

Abbreviations

CD, circular dichroism;

DFT, density functional theory;

DTT, dithiothreitol;

DNIC, dinitrosyl iron complex;

EPR, electron paramagnetic resonance;

ESI-MS, electrospray ionization mass spectrometry;

GSNO, S-nitrosoglutathione;

HTH, helix-turn-helix;

NO, nitric oxide;

NRVS, nuclear resonance vibrational spectroscopy;

RBE, Roussin’s black ester;

RBS, Roussin’s black salt;

RNS, reactive nitrogen species;

ROS, reactive oxygen species;

RRE, Roussin’s red ester;

SHE, standard hydrogen electrode.

Figure legends

Figure 1. Iron-sulfur clusters that are common in nature. Structures of [2Fe-2S], [3Fe-4S], and [4Fe-4S] iron sulfur clusters (PDB:1I7H (79), 2VKR (50)). Iron, sulfide, and cysteine residues are indicated. These and other structural images in this article were generated using UCSF Chimera (128).

Figure 2. Crystal structure of [4Fe-4S] FNR. A) Annotated structure of *Aliivibrio fischeri* FNR. Each subunit contains an N-terminal β-roll sensory domain that binds an all Cys ligated [4Fe-4S] cluster (shown as space filled). **B)** The [4Fe-4S] cluster binding loop in more detail. The location of cluster ligands (Cys20, 23, 29, and 122) and residues known to affect O_2 sensitivity are indicated (PDB: 5E44 (176)).

Figure 3. ESI-MS of [4Fe-4S] FNR and the effect of O_2. **A)** Representative deconvoluted mass spectra of [4Fe-4S] S24F FNR before (0 min) and after (up to 20 min) exposure to dissolved atmospheric O_2. This results in the formation of a variety of protein bound clusters, including [3Fe-4S], [3Fe-3S] and [2Fe-2S] clusters. Persulfide adducts of [2Fe-2S] and apo-protein are also observed. **B)** Plots of relative abundance of [4Fe-4S] cluster (derived from $A_{406\ nm}$, black squares), [3Fe-4S] / [3Fe-3S](S) (yellow triangles), [3Fe-3S] (blue circles) and [2Fe-2S] cluster (red diamonds) species as a function of time following O_2 exposure. Fits derived from a global analysis of the experimental data are shown as solid lines. Data are from (33). **C)** Deconvoluted mass spectra of natural abundance (black lines) and isotopically labeled (^{34}S) sulfur (blue lines) forms of [4Fe-4S] S24F FNR and cluster conversion intermediates/products, as indicated.

Figure 4. Schematic model of *E. coli* FNR regulation. Scheme summarizing the mechanism of the reaction of [4Fe-4S] FNR with O_2. Dimeric holo-FNR is required for the expression of the *narGHJI* operon. Exposure to O_2 initiates iron-sulfur cluster conversion,

which pauses at [2Fe-2S] cluster forms and results in separation into monomers and loss of DNA binding. Consequently, expression of *nar* operon is downregulated. It is not currently known whether the transiently formed [3Fe-4S] form is transcriptionally active. If anaerobic conditions return, [2Fe-2S] or apo-FNR can be restored to [4Fe-4S] FNR via the *isc* FeS assembly system, restoring *nar* expression. (PDB: 5E44, 5CVR (176)).

Figure 5. Schematic model of the NreACB regulatory system. Under anaerobic conditions NreB acquires an O_2 sensitive [4Fe-4S] cluster. In the absence of nitrate (NO_3^-), NreA binds to NreB inhibiting its phosphorylation activity. In the presence of nitrate, NreA[NO_3^-] is formed, the interaction with NreB is decreased and the inhibitory effect on NreB phosphorylation activity is lost. NreC is a substrate for the NreB kinase domain. Phosphorylated (P) NreC is competent for DNA binding, resulting in an increased in *narG* expression. Depletion of nitrate or the return of oxygen inhibit the kinase activity of NreB.

Figure 6. Crystal structure of [2Fe-2S] SoxR A) Annotated structure of *Escherichia coli* SoxR, containing a C-terminal [2Fe-2S] cluster (shown as space filled). Inset, surface view of cluster binding loop highlighting the solvent exposed nature of the cluster (PDB: 2ZHG (181) and UCSF Chimeria). **B)** Schematic model of *E. coli* SoxRS regulatory system. DNA binding of [2Fe-2S] SoxR has been reported for oxidized (2+) and reduced (1+) forms. The cluster is maintained in the reduced state, $[2Fe\text{-}2S]^{1+}$, by the NADPH dependent *rsx* system. Oxidation of the cluster, to $[2Fe\text{-}2S]^{2+}$, through direct interaction with redox cycling drugs (or perturbations to the NADP/NADPH pool) activates the transcription of *soxS*, which in turn activates transcription of the SoxS operon. Note, a high-resolution structure of *E. coli* SoxS is not yet available. The schematic representation included here is based on the published structure of an AraC/XylS family protein (PDB: 1D5Y (96)), which shares 56% homology with SoxS (3,52).

Figure 7. Types of iron nitrosyl species formed during iron-sulfur cluster nitrosylation. The well characterised small molecule iron-nitrosyl species dinitrosyl iron complex (DNIC), Roussin's red ester (RRE), and Roussin's black salt (RBS) are illustrated. Also shown is a putative Roussin's black ester (RBE) species that could result from replacement of sulfide in RBS with one or more thiolate bridges. Other related nitrosyl species are also possible and are reviewed in (21,104).

Figure 8. Crystal structure of [4Fe-4S] NsrR. A) *S. coelicolor* NsrR is a homo-dimer, composed of elongated monomeric subunits. Each subunits contains an N-terminal DNA binding domain (helices 1-3), a long dimerization helix, and a C-terminal loop that binds the [4Fe-4S] cluster. **B)** The [4Fe-4S] cluster binding loop in more detail. The location of the Cys ligands (residues 93, 99, and 105) is shown. The fourth ligand, Asp8, originates from helix 1 of the opposite monomer (PDB: 5N07 (177)).

Figure 9. A regulatory model for *S. coelicolor* NsrR. A) 2D representation of the near-cluster residue interaction network. Arg12 from helix 1 connects to Asp8 on the same helix and Val36 from helix 2. Gly37 from helix 2 forms an inter-subunit connection with Asn97 in the cluster-binding loop. Glu85 connects helix 5 with Thr7 and Thr4 from helix 1. These interactions, together with the [4Fe-4S] cluster, correctly position the recognition helix (helix 3) for optimal DNA binding (PDB: 5N07). **B)** Comparison of holo- and apo-NsrR structures. Note, the increased length compared to holo-NsrR of the dimerization helix (DI) and C-terminal lengthening of helix 5 (*) of apo-NsrR to include cluster ligating Cys residues (PDB 5N08). RH, recognition helix. **C)** Scheme summarizing the mechanism of NsrR NO-sensing and regulation. Holo-NsrR binds to promotor sequences upstream of *hmpA1/2* genes (encoding flavohemoglobin NO dioxygenases), repressing expression. Detection of NO by the iron-sulfur cluster leads to a loss of DNA binding, allowing expression of *hmpA1/2* in an NO responsive manner. Note, a high-resolution structure of *E. coli* Hmp is not yet available. The schematic includes the structure of flavohemoglobin (PDB 1CQX), and putative NO dioxygenase, from

A. eutrophus (42). The heme and flavin-adenine dinucleotide cofactors present in 1CQX are space filled.

References

1. Achebach S, Selmer T, and Unden G. Properties and significance of apoFNR as a second form of air-inactivated [4Fe-4S] FNR of *Escherichia coli*. *FEBS J* 272: 4260-4269, 2005.
2. Alam MS, Garg SK, and Agrawal P. Studies on structural and functional divergence among seven WhiB proteins of *Mycobacterium tuberculosis* H37Rv. *FEBS J* 276: 76-93, 2009.
3. Altschul SF, Madden TL, Schaffer AA, Zhang J, Zhang Z, Miller W, Lipman DJ. Gapped BLAST and PSI-BLAST: a new generation of protein database search programs. *Nucl Acids Res* 25: 3389-402, 1997.
4. Bailey S. Nuclear replication: Hidden iron-sulfur clusters. *Nat Chem Biol* 8: 24-25, 2011.
5. Bartolini E, Frigimelica E, Giovinazzi S, Galli G, Shaik Y, Genco C, Welsch JA, Granoff DM, Grandi G, and Grifantini R. Role of FNR and FNR-regulated, sugar fermentation genes in *Neisseria meningitidis* infection. *Mol Microbiol* 60: 963-972, 2006.
6. Bates DM, Lazazzera BA, and Kiley PJ. Characterization of FNR* mutant proteins indicates two distinct mechanisms for altering oxygen regulation of the *Escherichia coli* transcription factor FNR. *J Bacteriol* 177: 3972-3978, 1995.
7. Bates DM, Popescu CV, Khoroshilova N, Vogt K, Beinert H, Munck E, and Kiley PJ. Substitution of leucine 28 with histidine in the *Escherichia coli* transcription factor FNR results in increased stability of the $[4Fe\text{-}4S]^{2+}$ cluster to oxygen. *J Biol Chem* 275: 6234-6240, 2000.
8. Becker S, Holighaus G, Gabrielczyk T, and Unden G. O_2 as the regulatory signal for FNR-dependent gene regulation in *Escherichia coli*. *J Bacteriol* 178: 4515-4521, 1996.
9. Beinert H, Holm RH, and Munck E. Iron-sulfur clusters: Nature's modular, multipurpose structures. *Science* 277: 653-659, 1997.

10. Beinert H, Kennedy MC, and Stout CD. Aconitase as iron-sulfur protein, enzyme, and iron-regulatory protein. *Chem Rev* 96: 2335-2374, 1996.

11. Benjamin JA and Masse E. The iron-sensing aconitase B binds its own mRNA to prevent sRNA-induced mRNA cleavage. *Nucleic Acids Res* 42: 10023-36, 2014.

12. Bergaust L, van Spanning RJ, Frostegard A, and Bakken LR. Expression of nitrous oxide reductase in *Paracoccus denitrificans* is regulated by oxygen and nitric oxide through FnrP and NNR. *Microbiology* 158: 826-834, 2012.

13. Bian SM and Cowan JA. Protein-bound iron-sulfur centers. Form, function, and assembly. *Coord Chem Rev* 192: 1049-1066, 1999.

14. Bouton C, Oliveira L, and Drapier JC. Converse modulation of IRP1 and IRP2 by immunological stimuli in murine RAW 264.7 macrophages. *J Biol Chem* 273: 9403-9408, 1998.

15. Bradley TM, Hidalgo E, Leautaud V, Ding H, and Demple B. Cysteine-to-alanine replacements in the *Escherichia coli* SoxR protein and the role of the [2Fe-2S] centers in transcriptional activation. *Nucleic Acids Res* 25: 1469-1475, 1997.

16. Brereton PS, Duderstadt RE, Staples CR, Johnson MK, Adams MW. Effect of serinate ligation at each of the iron sites of the [Fe_4S_4] cluster of *Pyrococcus furiosus* ferredoxin on the redox, spectroscopic, and biological properties. *Biochemistry* 38: 10594-605, 1999.

17. Burian J, Ramon-Garcia S, Howes CG, and Thompson CJ. WhiB7, a transcriptional activator that coordinates physiology with intrinsic drug resistance in *Mycobacterium tuberculosis*. *Expert Rev Anti Infect Ther* 10: 1037-1047, 2012.

18. Burian J, Yim G, Hsing M, Axerio-Cilies P, Cherkasov A, Spiegelman GB, and Thompson CJ. The mycobacterial antibiotic resistance determinant WhiB7 acts as a transcriptional activator by binding the primary sigma factor SigA (RpoV). *Nucleic Acids Res* 41: 10062-76, 2013.

19. Bus JS and,Gibson JE. Paraquat: model for oxidant-initiated toxicity. *Environ Health Perspect* 55: 37-46, 1984.

20. Bush MJ, Chandra G, Bibb MJ, Findlay KC, and Buttner MJ. Genome-wide chromatin immunoprecipitation sequencing analysis shows that WhiB is a transcription factor that co-controls its regulon with WhiA to initiate developmental cell division in *Streptomyces*. *MBio* 7: e00523-16, 2016.

21. Butler AR, Glidewell C, and Li M. Nitrosyl complexes of iron-sulfur clusters. *Adv Inorg Chem* 32: 335-393, 1988.

22. Casonato S, Cervantes Sanchez A, Haruki H, Rengifo Gonzalez M, Provvedi R, Dainese E, Jaouen T, Gola S, Bini E, Vicente M, Johnsson K, Ghisotti D, Palu G, Hernandez-Pando R, and Manganelli R. WhiB5, a transcriptional regulator that contributes to *Mycobacterium tuberculosis* virulence and reactivation. *Infect Immun* 80: 3132-3144, 2012.

23. Chen Z, Hu Y, Cumming BM, Lu P, Feng L, Deng J, Steyn AJ, and Chen S. Mycobacterial WhiB6 differentially regulates ESX-1 and the Dos regulon to modulate granuloma formation and virulence in zebrafish. *Cell Rep* 16: 2512-2524, 2016.

24. Crack J, Green J, and Thomson AJ. Mechanism of oxygen sensing by the bacterial transcription factor fumarate-nitrate reduction (FNR). *J Biol Chem* 279: 9278-9286, 2004.

25. Crack JC, Gaskell AA, Green J, Cheesman MR, Le Brun NE, and Thomson AJ. Influence of the environment on the $[4Fe\text{-}4S]^{2+}$ to $[2Fe\text{-}2S]^{2+}$ cluster switch in the transcriptional regulator FNR. *J Am Chem Soc* 130: 1749-1758, 2008.

26. Crack JC, Green J, Cheesman MR, Le Brun NE, and Thomson AJ. Superoxide-mediated amplification of the oxygen-induced switch from [4Fe-4S] to [2Fe-2S] clusters in the transcriptional regulator FNR. *Proc Natl Acad Sci U S A* 104: 2092-2097, 2007.

27. Crack JC, Green J, Hutchings MI, Thomson AJ, and Le Brun NE. Bacterial iron-sulfur regulatory proteins as biological sensor-switches. *Antioxid Redox Signal* 17: 1215-1231, 2012.

28. Crack JC, Hutchings MI, Thomson AJ, and Le Brun NE. Biochemical properties of *Paracoccus denitrificans* FnrP: reactions with molecular oxygen and nitric oxide. *J Biol Inorg Chem* 21: 71-82, 2016.

29. Crack JC, Munnoch J, Dodd EL, Knowles F, Al Bassam MM, Kamali S, Holland AA, Cramer SP, Hamilton CJ, Johnson MK, Thomson AJ, Hutchings MI, and Le Brun NE. NsrR from *Streptomyces coelicolor* is a nitric oxide-sensing [4Fe-4S] cluster protein with a specialized regulatory function. *J Biol Chem* 290: 12689-704, 2015.

30. Crack JC, Smith LJ, Stapleton MR, Peck J, Watmough NJ, Buttner MJ, Buxton RS, Green J, Oganesyan VS, Thomson AJ, and Le Brun NE. Mechanistic insight into the nitrosylation of the [4Fe-4S] Cluster of WhiB-like proteins. *J Am Chem Soc* 133: 1112-1121, 2011.

31. Crack JC, Stapleton MR, Green J, Thomson AJ, and Le Brun NE. Mechanism of $[4Fe\text{-}4S](Cys)_4$ cluster nitrosylation is conserved among NO-responsive regulators. *J Biol Chem* 288: 11492-11502, 2013.

32. Crack JC, Svistunenko DA, Munnoch J, Thomson AJ, Hutchings MI, and Le Brun NE. Differentiated, promoter-specific response of [4Fe-4S] NsrR DNA binding to reaction with nitric oxide. *J Biol Chem* 291: 8663-8672, 2016.

33. Crack JC, Thomson AJ, and Le Brun NE. Mass spectrometric identification of intermediates in the O_2 driven [4Fe-4S] to [2Fe-2S] cluster conversion in FNR. *Proc Natl Acad Sci U S A* 114:E3215-E3223, 2017.

34. Davis NK and Chater KF. The *Streptomyces coelicolor whiB* gene encodes a small transcription factor-like protein dispensable for growth but essential for sporulation. *Mol Gen Genet* 232: 351-358, 1992.

35. den Hengst CD and Buttner MJ. Redox control in Actinobacteria. *Biochim Biophys Acta* 1780: 1201-1216, 2008.

36. Dibden DP and Green J. *In vivo* cycling of the *Escherichia coli* transcription factor FNR between active and inactive states. *Microbiology* 151: 4063-4070, 2005.

37. Ding H and,Demple B. Direct nitric oxide signal transduction via nitrosylation of iron-sulfur centers in the SoxR transcription activator. *Proc Natl Acad Sci U S A* 97: 5146-50, 2000.

38. Dunn AK, Karr EA, Wang Y, Batton AR, Ruby EG, and Stabb EV. The alternative oxidase (AOX) gene in *Vibrio fischeri* is controlled by NsrR and upregulated in response to nitric oxide. *Mol Microbiol* 77: 44-55, 2010.

39. Dupuy J, Volbeda A, Carpentier P, Darnault C, Moulis JM, and Fontecilla-Camps JC. Crystal structure of human iron regulatory protein 1 as cytosolic aconitase. *Structure* 14: 129-139, 2006.

40. Edwards J, Cole LJ, Green JB, Thomson MJ, Wood AJ, Whittingham JL, and Moir JW. Binding to DNA protects *Neisseria meningitidis* fumarate and nitrate reductase regulator (FNR) from oxygen. *J Biol Chem* 285: 1105-12, 2010.

41. Eriksson S, Lucchini S, Thompson A, Rhen M, and Hinton JC. Unravelling the biology of macrophage infection by gene expression profiling of intracellular *Salmonella enterica*. *Mol Microbiol* 47: 103-18, 2003.

42. Ermler U, Siddiqui RA, Cramm R, and Friedrich B. Crystal structure of the flavohemoglobin from *Alcaligenes eutrophus* at 1.75 A resolution. *EMBO J* 14: 6067-77, 1995.

43. Facey PD, Sevcikova B, Novakova R, Hitchings MD, Crack JC, Kormanec J, Dyson PJ and Del Sol R. The *dpsA* gene of *Streptomyces coelicolor*: induction of expression from a single promoter in response to environmental stress or during development. *PLoS One* 6: e25593, 2011.

44. Fang FC, Vazquez-Torres A and Xu Y. The transcriptional regulator SoxS is required for resistance of *Salmonella typhimurium* to paraquat but not for virulence in mice. *Infect Immun* 65: 5371-5, 1997.

45. Fedtke I, Kamps A, Krismer B and Gotz F. The nitrate reductase and nitrite reductase operons and the *narT* gene of *Staphylococcus carnosus* are positively controlled by the novel two-component system NreBC. *J Bacteriol* 184: 6624-34, 2002.

46. Filenko N, Spiro S, Browning DF, Squire D, Overton TW, Cole J and Constantinidou C. The NsrR regulon of *Escherichia coli* K-12 includes genes encoding the hybrid cluster protein and the periplasmic, respiratory nitrite reductase. *J Bacteriol* 189: 4410-7, 2007.

47. Fink RC, Evans MR, Porwollik S, Vazquez-Torres A, Jones-Carson J, Troxell B, Libby SJ, McClelland M and Hassan HM. FNR is a global regulator of virulence and anaerobic metabolism in *Salmonella enterica* serovar typhimurium (ATCC 14028s). *J Bacteriol* 189: 2262-2273, 2007.

48. Flatley J, Barrett J, Pullan ST, Hughes MN, Green J, and Poole RK. Transcriptional responses of *Escherichia coli* to S-nitrosoglutathione under defined chemostat conditions reveal major changes in methionine biosynthesis. *J Biol Chem* 280: 10065-72, 2005.

49. Fleischhacker AS, Stubna A, Hsueh KL, Guo Y, Teter SJ, Rose JC, Brunold TC, Markley JL, Munck E and Kiley PJ. Characterization of the [2Fe-2S] cluster of *Escherichia coli* transcription factor IscR. *Biochemistry* 51: 4453-4462, 2012.

50. Frazao C, Aragao D, Coelho R, Leal SS, Gomes CM, Teixeira M and Carrondo MA. Crystallographic analysis of the intact metal centres $[3Fe\text{-}4S]^{1+/0}$ and $[4Fe\text{-}4S]^{2+/1+}$ in a Zn^{2+} -containing ferredoxin. *FEBS Lett* 582: 763-767, 2008.

51. Fujikawa M, Kobayashi K and Kozawa T. Mechanistic studies on formation of the dinitrosyl iron complex of the [2Fe-2S] cluster of SoxR protein. *J Biochem* 156: 163-172, 2014.

52. Gallegos MT, Schleif R, Bairoch A, Hofmann K, Ramos JL. Arac/XylS family of transcriptional regulators. *Microbiol Mol Biol Rev* 61: 393-410, 1997.

53. Garg S, Alam MS, Bajpai R, Kishan KR and Agrawal P. Redox biology of *Mycobacterium tuberculosis* H37Rv: protein-protein interaction between GlgB and WhiB1 involves exchange of thiol-disulfide. *BMC Biochem* 10: 1, 2009.

54. Garg SK, Alam MS, Soni V, Kishan KVR and Agrawal P. Characterization of *Mycobacterium tuberculosis* WhiB1/Rv3219 as a protein disulfide reductase. *Prot Exp Purif* 52: 422-432, 2007.

55. Gaudu P, Dubrac S and Touati D. Activation of SoxR by overproduction of desulfoferrodoxin: multiple ways to induce the *soxRS* regulon. *J Bacteriol* 182: 1761-3, 2000.

56. Gilberthorpe NJ, Lee ME, Stevanin TM, Read RC and Poole RK. NsrR: a key regulator circumventing *Salmonella enterica* serovar Typhimurium oxidative and nitrosative stress *in vitro* and in IFN-gamma-stimulated J774.2 macrophages. *Microbiology* 153: 1756-71, 2007.

57. Gorbunov KY, Laikova ON, Rodionov DA, Gelfand MS and Lyubetsky VA. Evolution of regulatory motifs of bacterial transcription factors. *In Silico Biol* 10: 163-183, 2010.

58. Gorodetsky AA, Dietrich LEP, Lee PE, Demple B, Newman DK and Barton JK. DNA binding shifts the redox potential of the transcription factor SoxR. *Proc Natl Acad Sci U S A* 105: 3684-3689, 2008.

59. Green J, Sharrocks AD, Green B, Geisow M and Guest JR. Properties of the FNR proteins substituted at each of the 5 cysteine residues. *Mol Microbiol* 8: 61-68, 1993.

60. Gruner I, Fradrich C, Bottger LH, Trautwein AX, Jahn D and Hartig E. Aspartate 141 is the fourth ligand of the oxygen-sensing $[4Fe\text{-}4S]^{2+}$ cluster of *Bacillus subtilis* transcriptional regulator Fnr. *J Biol Chem* 286: 2017-2021, 2011.

61. Gu MZ and Imlay JA. The SoxRS response of *Escherichia coli* is directly activated by redox-cycling drugs rather than by superoxide. *Mol Microbiol* 79: 1136-1150, 2011.

62. Guest JR. Oxygen-regulated gene expression in *Escherichia coli*. *J Gen Microbiol* 138: 2253-2263, 1992.

63. Guest JR. Adaptation to life without oxygen. *Philos Trans R Soc Lond B Biol Sci* 350: 189-202, 1995.

64. Gusarov I, Shatalin K, Starodubtseva M and Nudler E. Endogenous nitric oxide protects bacteria against a wide spectrum of antibiotics. *Science* 325: 1380-1384, 2009.

65. Gusarov I, Starodubtseva M, Wang ZQ, McQuade L, Lippard SJ, Stuehr DJ and Nudler E. Bacterial nitric-oxide synthases operate without a dedicated redox partner. *J Biol Chem* 283: 13140-13147, 2008.

66. Harel A, Bromberg Y and Falkowski PG, Bhattacharya D. Evolutionary history of redox metal-binding domains across the tree of life. *Proc Natl Acad Sci U S A* 111: 7042-7047, 2014.

67. Hartig E and Jahn D. Regulation of the anaerobic metabolism in *Bacillus subtilis*. *Adv Microb Physiol* 61: 195-216, 2012.

68. Hunsicker-Wang LM, Heine A, Chen Y, Luna EP, Todaro T, Zhang YM, Williams PA, McRee DE, Hirst J, Stout CD, Fee JA. High-resolution structure of the soluble, respiratory-type Rieske protein from *Thermus thermophilus*: analysis and comparison. *Biochemistry* 42: 7303-17, 2003.

69. Hutchings MI, Crack JC, Shearer N, Thompson BJ, Thomson AJ and,Spiro S. Transcription factor FnrP from *Paracoccus denitrificans* contains an iron-sulfur cluster and is activated by anoxia: Identification of essential cysteine residues. *J Bacteriol* 184: 503-508, 2002.

70. Imlay JA. Cellular defenses against superoxide and hydrogen peroxide. *Ann Rev Biochem* 77: 755-776, 2008.

71. Jakimowicz P, Cheesman MR, Bishai WR, Chater KF, Thomson AJ and Buttner MJ. Evidence that the *Streptomyces* developmental protein WhiD, a member of the WhiB family, binds a [4Fe-4S] cluster. *J Biol Chem* 280: 8309-8315, 2005.

72. Jervis AJ, Crack JC, White G, Artymiuk PJ, Cheesman MR, Thomson AJ, Le Brun NE and,Green J. The O_2 sensitivity of the transcription factor FNR is controlled by Ser24 modulating the kinetics of [4Fe-4S] to [2Fe-2S] conversion. *Proc Natl Acad Sci U S A* 106: 4659-4664, 2009.

73. Johnson KA, Verhagen MFJM, Brereton PS, Adams MWW and Amster IJ. Probing the stoichiometry and oxidation states of metal centers in iron-sulfur proteins using electrospray FTICR mass spectrometry. *Anal Chem* 72: 1410-1418, 2000.

74. Johnson MK. Iron-sulfur proteins: new roles for old clusters. *Curr Opin Chem Biol* 2: 173-81, 1998.

75. Jordan PA, Tang Y, Bradbury AJ, Thomson AJ and Guest JR. Biochemical and spectroscopic characterization of *Escherichia coli* aconitases (AcnA and AcnB). *Biochem J* 344: 739-746, 1999.

76. Jung JY, Madan-Lala R, Georgieva M, Rengarajan J, Sohaskey CD, Bange FC and Robinson CM. The intracellular environment of human macrophages that produce nitric oxide promotes growth of mycobacteria. *Infect Immun* 81: 3198-3209, 2013.

77. Kaiser BK, Clifton MC, Shen BW and Stoddard BL. The structure of a bacterial DUF199/WhiA protein: domestication of an invasive endonuclease. *Structure* 17: 1368-1376, 2009.

78. Kaiser BK and Stoddard BL. DNA recognition and transcriptional regulation by the WhiA sporulation factor. *Sci Rep* 1: 156, 2011.

79. Kakuta Y, Horio T, Takahashi Y and Fukuyama K. Crystal structure of *Escherichia coli* Fdx, an adrenodoxin-type ferredoxin involved in the assembly of iron-sulfur clusters. *Biochemistry* 40: 11007-11012, 2001.

80. Kamps A, Achebach S, Fedtke I, Unden G and Gotz F. *Staphylococcal* NreB: an O_2-sensing histidine protein kinase with an O_2-labile iron-sulphur cluster of the FNR type. *Mol Microbiol* 52: 713-723, 2004.

81. Karlinsey JE, Bang IS, Becker LA, Frawley ER, Porwollik S, Robbins HF, Thomas VC, Urbano R, McClelland M and Fang FC. The NsrR regulon in nitrosative stress resistance of *Salmonella enterica* serovar Typhimurium. *Mol Microbiol* 85: 1179-93, 2012.

82. Karp PD, Weaver D, Paley S, Fulcher C, Kubo A, Kothari A, Krummenacker M, Subhraveti P, Weerasinghe D, Gama-Castro S, Huerta AM, Muniz-Rascado L,

Bonavides-Martinez C, Weiss V, Peralta-Gil M, Santos-Zavaleta A, Schroder I, Mackie A, Gunsalus R, Collado-Vides J, Keseler IM and Paulsen I. The EcoCyc Database. *EcoSal Plus* 6, 2014.

83. Kennedy MC, Antholine WE and Beinert H. An EPR investigation of the products of the reaction of cytosolic and mitochondrial aconitases with nitric oxide. *J Biol Chem* 272: 20340-20347, 1997.

84. Khoroshilova N, Beinert H and Kiley PJ. Association of a polynuclear iron-sulfur cluster center with a mutant FNR protein enhances DNA-binding. *Proc Natl Acad Sci U S A* 92: 2499-2503, 1995.

85. Khoroshilova N, Popescu C, Munck E, Beinert H and Kiley PJ. Iron-sulfur cluster disassembly in the FNR protein of *Escherichia coli* by O_2: [4Fe-4S] to [2Fe-2S] conversion with loss of biological activity. *Proc Natl Acad Sci U S A* 94: 6087-6092, 1997.

86. Kiley PJ and Beinert H. Oxygen sensing by the global regulator, FNR: the role of the iron-sulfur cluster. *FEMS Microbiol Rev* 22: 341-352, 1999.

87. Kiley PJ and Beinert H. The role of Fe-S proteins in sensing and regulation in bacteria. *Curr Opin Microbiol* 6: 181-185, 2003.

88. Kiley PJ and Reznikoff WS. FNR mutants that activate gene expression in the presence of oxygen. *J Bacteriol* 173: 16-22, 1991.

89. Kobayashi K, Fujikawa M and Kozawa T. Binding of promoter DNA to SoxR protein decreases the reduction potential of the [2Fe-2S] cluster. *Biochemistry* 54: 334-339, 2015.

90. Kommineni S, Lama A, Popescu B and Nakano MM. Global transcriptional control by NsrR in *Bacillus subtilis*. *J Bacteriol* 194: 1679-88, 2012.

91. Kommineni S, Yukl E, Hayashi T, Delepine J, Geng H, Moenne-Loccoz P and Nakano MM. Nitric oxide-sensitive and -insensitive interaction of *Bacillus subtilis* NsrR with a ResDE-controlled promoter. *Mol Microbiol* 78: 1280-1293, 2010.

92. Konar M, Alam MS, Arora C and Agrawal P. WhiB2/Rv3260c, a cell division-associated protein of *Mycobacterium tuberculosis* H37Rv, has properties of a chaperone. *FEBS J* 279: 2781-92, 2012.

93. Koo MS, Lee JH, Rah SY, Yeo WS, Lee JW, Lee KL, Koh YS, Kang SO and Roe JH. A reducing system of the superoxide sensor SoxR in *Escherichia coli*. *EMBO J* 22: 2614-2622, 2003.

94. Krapp AR, Humbert MV, Carrillo N. The *soxRS* response of *Escherichia coli* can be induced in the absence of oxidative stress and oxygen by modulation of NADPH content. *Microbiology* 157: 957-65, 2011.

95. Krieglstein CF, Cerwinka WH, Laroux FS, Salter JW, Russell JM, Schuermann G, Grisham MB, Ross CR and Granger DN. Regulation of murine intestinal inflammation by reactive metabolites of oxygen and nitrogen: divergent roles of superoxide and nitric oxide. *J Exp Med* 194: 1207-1218, 2001.

96. Kwon HJ, Bennik MH, Demple B and Ellenberger T. Crystal structure of the Escherichia coli Rob transcription factor in complex with DNA. *Nat Struct Biol* 7: 424-430, 2000.

97. Lancaster KM, Roemelt M, Ettenhuber P, Hu Y, Ribbe MW, Neese F, Bergmann U and DeBeer S. X-ray emission spectroscopy evidences a central carbon in the nitrogenase iron-molybdenum cofactor. *Science* 334: 974-977, 2011.

98. Larsson C, Luna B, Ammerman NC, Maiga M, Agarwal N and Bishai WR. Gene expression of *Mycobacterium tuberculosis* putative transcription factors WhiB1-7 in redox environments. *PLoS One* 7: e37516, 2012.

99. Laver JR, Stevanin TM, Messenger SL, Lunn AD, Lee ME, Moir JW, Poole RK and Read RC. Bacterial nitric oxide detoxification prevents host cell S-nitrosothiol formation: a novel mechanism of bacterial pathogenesis. *FASEB J* 24: 286-295, 2010.

100. Lazazzera BA, Bates DM and Kiley PJ. The activity of the *Escherichia coli* transcription factor FNR is regulated by a change in oligomeric state. *Genes Dev* 7: 1993-2005, 1993.

101. Lazazzera BA, Beinert H, Khoroshilova N, Kennedy MC and Kiley PJ. DNA binding and dimerization of the Fe-S-containing FNR protein from *Escherichia coli* are regulated by oxygen. *J Biol Chem* 271: 2762-2768, 1996.

102. Lee Y, Jeon IR, Abboud KA, Garcia-Serres R, Shearer J and Murray LJ. A $[3Fe\text{-}3S]^{3+}$ cluster with exclusively μ-sulfide donors. *Chem Commun* 52: 1174-1177, 2016.

103. Lee YY, Shearer N and Spiro S. Transcription factor NNR from *Paracoccus denitrificans* is a sensor of both nitric oxide and oxygen: isolation of *nnr** alleles encoding effector-independent proteins and evidence for a haem-based sensing mechanism. *Microbiology* 152: 1461-70, 2006.

104. Li L and Li L. Recent advances in multinuclear metal nitrosyl complexes. *Coord Chem Rev* 306: 678-700, 2016.

105. Lin J, Zhou T, Ye K, Wang J. Crystal structure of human mitoNEET reveals distinct groups of iron sulfur proteins. *Proc Natl Acad Sci U S A* 104: 14640-5, 2007.

106. Lo FC, Chen CL, Lee CM, Tsai MC, Lu TT, Liaw WF and Yu SSF. A study of NO trafficking from dinitrosyl-iron complexes to the recombinant E-coli transcriptional factor SoxR. *J Biol Inorg Chem* 13: 961-972, 2008.

107. Lo FC, Lee JF, Liaw WF, Hsu IJ, Tsai YF, Chan SI and Yu SS. The metal core structures in the recombinant *Escherichia coli* transcriptional factor SoxR. *Chemistry* 18: 2565-2577, 2012.

108. Macomber L and Imlay JA. The iron-sulfur clusters of dehydratases are primary intracellular targets of copper toxicity. *Proc Natl Acad Sci U S A* 106: 8344-8349, 2009.

109. Mansy SS, Xiong Y, Hemann C, Hille R, Sundaralingam M, Cowan JA. Crystal structure and stability studies of C77S HiPIP: a serine ligated [4Fe-4S] cluster. *Biochemistry* 41: 1195-201, 2002.

110. Marshall FA, Messenger SL, Wyborn NR, Guest JR, Wing H, Busby SJ and Green J. A novel promoter architecture for microaerobic activation by the anaerobic transcription factor FNR. *Mol Microbiol* 39: 747-53, 2001.

111. Marteyn B, West NP, Browning DF, Cole JA, Shaw JG, Palm F, Mounier J, Prevost MC, Sansonetti P and Tang CM. Modulation of *Shigella* virulence in response to available oxygen *in vivo*. *Nature* 465: 355-8, 2010.

112. McCollister BD, Hoffman M, Husain M and Vazquez-Torres A. Nitric oxide protects bacteria from aminoglycosides by blocking the energy-dependent phases of drug uptake. *Antimicrob Agents Chemother* 55: 2189-96, 2011.

113. Mehta M, Rajmani RS and Singh A. *Mycobacterium tuberculosis* WhiB3 responds to vacuolar pH-induced changes in mycothiol redox potential to modulate phagosomal maturation and virulence. *J Biol Chem* 291: 2888-2903, 2016.

114. Mettert EL and Kiley PJ. ClpXP-dependent proteolysis of FNR upon loss of its O_2-sensing [4Fe-4S] cluster. *J Mol Biol* 354: 220-232, 2005.

115. Mettert EL, Outten FW, Wanta B and Kiley PJ. The Impact of O_2 on the Fe-S cluster biogenesis requirements of *Escherichia coli* FNR. *J Mol Biol* 384: 798-811, 2008.

116. Molle V, Palframan WJ, Findlay KC and Buttner MJ. WhiD and WhiB, homologous proteins required for different stages of sporulation in *Streptomyces coelicolor* A3(2). *J Bacteriol* 182: 1286-1295, 2000.

117. Moore LJ and Kiley PJ. Characterization of the dimerization domain in the FNR transcription factor. *J Biol Chem* 276: 45744-45750, 2001.

118. Morris RP, Nguyen L, Gatfield J, Visconti K, Nguyen K, Schnappinger D, Ehrt S, Liu Y, Heifets L, Pieters J, Schoolnik G and Thompson CJ. Ancestral antibiotic resistance in *Mycobacterium tuberculosis*. *Proc Natl Acad Sci U S A* 102: 12200-12205, 2005.

119. Mullner M, Hammel O, Mienert B, Schlag S, Bill E and Unden G. A PAS domain with an oxygen labile $[4Fe\text{-}4S]^{2+}$ cluster in the oxygen sensor kinase NreB of *Staphylococcus carnosus*. *Biochemistry* 47: 13921-13932, 2008.

120. Munnoch JT, Martinez MT, Svistunenko DA, Crack JC, Le Brun NE and Hutchings MI. Characterization of a putative NsrR homologue in *Streptomyces venezuelae* reveals a new member of the Rrf2 superfamily. *Sci Rep* 6: 31597, 2016.

121. Nesbit AD, Giel JL, Rose JC and Kiley PJ. Sequence-specific binding to a subset of IscR-regulated promoters does not require IscR Fe-S cluster ligation. *J Mol Biol* 387: 28-41, 2009.

122. Nicolet Y, Rohac R, Martin L and Fontecilla-Camps JC. X-ray snapshots of possible intermediates in the time course of synthesis and degradation of protein-bound Fe4S4 clusters. *Proc Natl Acad Sci U S A* 110: 7188-92, 2013.

123. Niemann V, Koch-Singenstreu M, Neu A, Nilkens S, Gotz F, Unden G and Stehle T. The NreA protein functions as a nitrate receptor in the Staphylococcal nitrate regulation system. *J Mol Biol* 426: 1539-1553, 2014.

124. Nunoshiba T, DeRojas-Walker T, Tannenbaum SR and Demple B. Roles of nitric oxide in inducible resistance of *Escherichia coli* to activated murine macrophages. *Infect Immun* 63: 794-798, 1995.

125. Nunoshiba T, deRojas-Walker T, Wishnok JS, Tannenbaum SR and Demple B. Activation by nitric oxide of an oxidative-stress response that defends *Escherichia coli* against activated macrophages. *Proc Natl Acad Sci U S A* 90: 9993-9997, 1993.

126. Otten MF, Stork DM, Reijnders WN, Westerhoff HV, Van Spanning RJ. Regulation of expression of terminal oxidases in *Paracoccus denitrificans*. *Eur J Biochem* 268: 2486-2497, 2001.

127. Partridge JD, Bodenmiller DM, Humphrys MS and Spiro S. NsrR targets in the Escherichia coli genome: new insights into DNA sequence requirements for binding and a role for NsrR in the regulation of motility. *Mol Microbiol* 73: 680-694, 2009.

128. Pettersen EF, Goddard TD, Huang CC, Couch GS, Greenblatt DM, Meng EC and Ferrin TE. UCSF Chimera - a visualization system for exploratory research and analysis. *J Comput Chem* 25: 1605-1612, 2004.

129. Phillips JD, Kinikini DV, Yu Y, Guo B and Leibold EA. Differential regulation of IRP1 and IRP2 by nitric oxide in rat hepatoma cells. *Blood* 87: 2983-2992, 1996.

130. Pomposiello PJ and Demple B. Redox-operated genetic switches: the SoxR and OxyR transcription factors. *Trends Biotechnol* 19: 109-114, 2001.

131. Poole RK. Nitric oxide and nitrosative stress tolerance in bacteria. *Biochem Soc Trans* 33: 176-180, 2005.

132. Pullan ST, Gidley MD, Jones RA, Barrett J, Stevanin TM, Read RC, Green J and Poole RK. Nitric oxide in chemostat-cultured *Escherichia coli* is sensed by Fnr and other global regulators: unaltered methionine biosynthesis indicates lack of S nitrosation. *J Bacteriol* 189: 1845-1855, 2007.

133. Raghunand TR and Bishai WR. Mapping essential domains of *Mycobacterium smegmatis* WhmD: Insights into WhiB structure and function. *J Bacteriol* 188: 6966-6976, 2006.

134. Rajagopalan S, Teter SJ, Zwart PH, Brennan RG, Phillips KJ and Kiley PJ. Studies of IscR reveal a unique mechanism for metal-dependent regulation of DNA binding specificity. *Nat Struct Mol Biol* 20: 740-747, 2013.

135. Ramon-Garcia S, Ng C, Jensen PR, Dosanjh M, Burian J, Morris RP, Folcher M, Eltis LD, Grzesiek S, Nguyen L and Thompson CJ. WhiB7, an Fe-S-dependent transcription factor that activates species-specific repertoires of drug resistance determinants in Actinobacteria. *J Biol Chem* 288: 34514-34528, 2013.

136. Ranquet C, Ollagnier-de-Choudens S, Loiseau L, Barras F and Fontecave M. Cobalt stress in *Escherichia coli*. The effect on the iron-sulfur proteins. *J Biol Chem* 282: 30442-51, 2007.

137. Recalcati S, Minotti G and Cairo G. Iron regulatory proteins: from molecular mechanisms to drug development. *Antioxid Redox Signal* 13: 1593-1616, 2010.

138. Reents H, Gruner I, Harmening U, Bottger LH, Layer G, Heathcote P, Trautwein AX, Jahn D and Hartig E. *Bacillus subtilis* Fnr senses oxygen via a [4Fe-4S] cluster

coordinated by three cysteine residues without change in the oligomeric state. *Mol Microbiol* 60: 1432-1445, 2006.

139. Reinhart F, Achebach S, Koch T, Unden G. Reduced apo-fumarate nitrate reductase regulator (ApoFNR) as the major form of FNR in aerobically growing *Escherichia coli*. *J Bacteriol* 190: 879-886, 2008.

140. Richard-Greenblatt M, Bach H, Adamson J, Pena-Diaz S, Li W, Steyn AJ and Av-Gay Y. Regulation of ergothioneine biosynthesis and its effect on *Mycobacterium tuberculosis* growth and infectivity. *J Biol Chem* 290: 23064-23076, 2015.

141. Rybniker J, Nowag A, van Gumpel E, Nissen N, Robinson N, Plum G and Hartmann P. Insights into the function of the WhiB-like protein of mycobacteriophage TM4--a transcriptional inhibitor of WhiB2. *Mol Microbiol* 77: 642-657, 2010.

142. Saini V, Cumming BM, Guidry L, Lamprecht DA, Adamson JH, Reddy VP, Chinta KC, Mazorodze JH, Glasgow JN, Richard-Greenblatt M, Gomez-Velasco A, Bach H, Av-Gay Y, Eoh H, Rhee K and Steyn AJ. Ergothioneine maintains redox and bioenergetic homeostasis essential for drug susceptibility and virulence of *Mycobacterium tuberculosis*. *Cell Rep* 14: 572-585, 2016.

143. Saini V, Farhana A and Steyn AJ. *Mycobacterium tuberculosis* WhiB3: a novel iron-sulfur cluster protein that regulates redox homeostasis and virulence. *Antioxid Redox Signal* 16: 687-697, 2012.

144. Sasaki Y, Oguchi H, Kobayashi T, Kusama S, Sugiura R, Moriya K, Hirata T, Yukioka Y, Takaya N, Yajima S, Ito S, Okada K, Ohsawa K, Ikeda H, Takano H, Ueda K and Shoun H. Nitrogen oxide cycle regulates nitric oxide levels and bacterial cell signaling. *Sci Rep* 6: 22038, 2016.

145. Schwartz CJ, Djaman O, Imlay JA and Kiley PJ. The cysteine desulfurase, IscS, has a major role in *in vivo* Fe-S cluster formation in *Escherichia coli*. *Proc Natl Acad Sci U S A* 97: 9009-9014, 2000.

146. Serrano PN, Wang H, Crack JC, Prior C, Hutchings MI, Thomson AJ, Kamali S, Yoda Y, Zhao J, Hu MY, Alp EE, Oganesyan VS, Le Brun NE and Cramer SP. Nitrosylation

of nitric-oxide-sensing regulatory proteins containing [4Fe-4S] clusters gives rise to multiple iron-nitrosyl complexes. *Angew Chem Int Ed* 55: 14575-14579, 2016.

147. Shepard W, Soutourina O, Courtois E, England P, Haouz A and Martin-Verstraete I. Insights into the Rrf2 repressor family - the structure of CymR, the global cysteine regulator of *Bacillus subtilis*. *FEBS J* 278: 2689-2701, 2011.

148. Shin JH, Singh AK, Cheon DJ and Roe JH. Activation of the SoxR Regulon in *Streptomyces coelicolor* by the extracellular form of the pigmented antibiotic actinorhodin. *J Bacteriol* 193: 75-81, 2011.

149. Shomura Y, Yoon KS, Nishihara H and Higuchi Y. Structural basis for a [4Fe-3S] cluster in the oxygen-tolerant membrane-bound [NiFe]-hydrogenase. *Nature* 479: 253-256, 2011.

150. Siedler S, Schendzielorz G, Binder S, Eggeling L, Bringer S and Bott M. SoxR as a single-cell biosensor for NADPH-consuming enzymes in *Escherichia coli*. *ACS Synth Biol* 3: 41-47, 2014.

151. Singh A, Crossman DK, Mai D, Guidry L, Voskuil MI, Renfrow MB and Steyn AJ. *Mycobacterium tuberculosis* WhiB3 maintains redox homeostasis by regulating virulence lipid anabolism to modulate macrophage response. *PLoS Pathog* 5: e1000545, 2009.

152. Singh A, Guidry L, Narasimhulu KV, Mai D, Trombley J, Redding KE, Giles GI, Lancaster JR and Steyn AJC. *Mycobacterium tuberculosis* WhiB3 responds to O_2 and nitric oxide via its [4Fe-4S] cluster and is essential for nutrient starvation survival. *Proc Natl Acad Sci U S A* 104: 11562-11567, 2007.

153. Singh AK, Shin JH, Lee KL, Imlay JA and Roe JH. Comparative study of SoxR activation by redox-active compounds. *Mol Microbiol* 90: 983-996, 2013.

154. Smith LJ, Stapleton MR, Buxton RS and Green J. Structure-function relationships of the *Mycobacterium tuberculosis* transcription factor WhiB1. *PLoS One* 7: e40407, 2012.

155. Smith LJ, Stapleton MR, Fullstone GJ, Crack JC, Thomson AJ, Le Brun NE, Hunt DM, Harvey E, Adinolfi S, Buxton RS and Green J. *Mycobacterium tuberculosis* WhiB1 is an essential DNA-binding protein with a nitric oxide-sensitive iron-sulfur cluster. *Biochem J* 432: 417-427, 2010.

156. Soliveri JA, Gomez J, Bishai WR and Chater KF. Multiple paralogous genes related to the *Streptomyces coelicolor* developmental regulatory gene *whiB* are present in *Streptomyces* and other Actinomycetes. *Microbiology* 146: 333-343, 2000.

157. Spiro S. Regulators of bacterial responses to nitric oxide. *FEMS Microbiol Rev* 31: 193-211, 2007.

158. Steyn AJ, Collins DM, Hondalus MK, Jacobs WR, Jr., Kawakami RP and Bloom BR. *Mycobacterium tuberculosis* WhiB3 interacts with RpoV to affect host survival but is dispensable for *in vivo* growth. *Proc Natl Acad Sci U S A* 99: 3147-3152, 2002.

159. Stys A, Galy B, Starzynski RR, Smuda E, Drapier JC, Lipinski P and Bouton C. Iron regulatory protein 1 outcompetes iron regulatory protein 2 in regulating cellular iron homeostasis in response to nitric oxide. *J Biol Chem* 286: 22846-22854, 2011.

160. Sutton VR, Mettert EL, Beinert H and Kiley PJ. Kinetic analysis of the oxidative conversion of the $[4Fe\text{-}4S]^{2+}$ cluster of FNR to a $[2Fe\text{-}2S]^{2+}$ cluster. *J Bacteriol* 186: 8018-8025, 2004.

161. Sutton VR, Stubna A, Patschkowski T, Munck E, Beinert H and Kiley PJ. Superoxide destroys the $[2Fe\text{-}2S]^{2+}$ cluster of FNR from *Escherichia coli*. *Biochemistry* 43: 791-798, 2004.

162. Tang Y and Guest JR. Direct evidence for mRNA binding and post-transcriptional regulation by *Escherichia coli* aconitases. *Microbiology* 145: 3069-3079, 1999.

163. Tang Y, Quail MA, Artymiuk PJ, Guest JR and Green J. *Escherichia coli* aconitases and oxidative stress: post-transcriptional regulation of *sodA* expression. *Microbiology* 148: 1027-1037, 2002.

164. Tanous C, Soutourina O, Raynal B, Hullo MF, Mervelet P, Gilles AM, Noirot P, Danchin A, England P and Martin-Verstraete I. The CymR regulator in complex with

the enzyme CysK controls cysteine metabolism in *Bacillus subtilis*. *J Biol Chem* 283: 35551-35560, 2008.

165. Todd JD, Wexler M, Sawers G, Yeoman KH, Poole PS and Johnston AWB. RirA, an iron-responsive regulator in the symbiotic bacterium *Rhizobium leguminosarum*. *Microbiology* 148: 4059-4071, 2002.

166. Toledo JC, Jr. and Augusto O. Connecting the chemical and biological properties of nitric oxide. *Chem Res Toxicol* 25: 975-989, 2012.

167. Torres MJ, Simon J, Rowley G, Bedmar EJ, Richardson DJ, Gates AJ and Delgado MJ. Nitrous oxide metabolism in nitrate-reducing bacteria: physiology and regulatory mechanisms. *Adv Microb Physiol* 68: 353-432, 2016.

168. Tucker NP, Hicks MG, Clarke TA, Crack JC, Chandra G, Le Brun NE, Dixon R and Hutchings MI. The transcriptional repressor protein NsrR senses nitric oxide directly via a [2Fe-2S] cluster. *Plos One* 3: e3623, 2008.

169. Unden G and Bongaerts J. Alternative respiratory pathways of *Escherichia coli*: energetics and transcriptional regulation in response to electron acceptors. *Biochim Biophys Acta* 1320: 217-234, 1997.

170. Unden G and Guest JR. Isolation and characterization of the FNR protein, the transcriptional regulator of anaerobic electron-transport in *Escherichia coli*. *Eur J Biochem* 146: 193-199, 1985.

171. Vanin AF. Dinitrosyl iron complexes with thiolate ligands: physico-chemistry, biochemistry and physiology. *Nitric Oxide* 21: 1-13, 2009.

172. Vanin AF, Borodulin RR and Mikoyan VD. Dinitrosyl iron complexes with natural thiol-containing ligands in aqueous solutions: Synthesis and some physico-chemical characteristics (A methodological review). *Nitric Oxide*, 2017. doi: 10.1016/j.niox.2017.02.005.

173. Varghese S, Tang Y and Imlay JA. Contrasting sensitivities of *Escherichia coli* aconitases A and B to oxidation and iron depletion. *J Bacteriol* 185: 221-230, 2003.

174. Vergara-Irigaray M, Fookes MC, Thomson NR and Tang CM. RNA-seq analysis of the influence of anaerobiosis and FNR on *Shigella flexneri*. *BMC Genomics* 15: 438, 2014.

175. Vine CE and Cole JA. Unresolved sources, sinks, and pathways for the recovery of enteric bacteria from nitrosative stress. *FEMS Microbiol Lett* 325: 99-107, 2011.

176. Volbeda A, Darnault C, Renoux O, Nicolet Y and Fontecilla-Camps JC. The crystal structure of the global anaerobic transcriptional regulator FNR explains its extremely fine-tuned monomer-dimer equilibrium. *Sci Adv* 1: e1501086, 2015.

177. Volbeda A, Dodd EL, Darnault C, Crack JC, Renoux O, Hutchings MI, Le Brun NE and Fontecilla-Camps JC. Crystal structures of apo and holo forms of the nitric oxide sensor regulator NsrR reveal the role of the [4Fe-4S] cluster in modulating DNA binding. *Nat Commun* 8:15052, 2017.

178. Volz K. The functional duality of iron regulatory protein 1. *Curr Opin Struct Biol* 18: 106-111, 2008.

179. Walden WE, Selezneva AI, Dupuy J, Volbeda A, Fontecilla-Camps JC, Theil EC and Volz K. Structure of dual function iron regulatory protein 1 complexed with ferritin IRE-RNA. *Science* 314: 1903-1908, 2006.

180. Wang Y, Cui T, Zhang C, Yang M, Huang YX, Li WH, Zhang L, Gao CH, He Y, Li YQ, Huang F, Zeng JM, Huang C, Yang QO, Tian YX, Zhao CC, Chen HC, Zhang H and He ZG. Global protein-protein interaction network in the human pathogen *Mycobacterium tuberculosis* H37Rv. *J Prot Res* 9: 6665-6677, 2010.

181. Watanabe S, Kita A, Kobayashi K and Miki K. Crystal structure of the [2Fe-2S] oxidative-stress sensor SoxR bound to DNA. *Proc Natl Acad Sci U S A* 105: 4121-4126, 2008.

182. Wink DA and Mitchell JB. Chemical biology of nitric oxide: Insights into regulatory, cytotoxic, and cytoprotective mechanisms of nitric oxide. *Free Radic Biol Med* 25: 434-456, 1998.

183. Xiong L, Yang Y, Ye YN, Teng JL, Chan E, Watt RM, Guo FB, Lau SK and Woo PC. *Laribacter hongkongensis* anaerobic adaptation mediated by arginine metabolism is controlled by the cooperation of FNR and ArgR. *Environ Microbiol*, 19:1266-1280, 2016.

184. Yoo JS, Oh GS, Ryoo S and Roe JH. Induction of a stable sigma factor SigR by translation-inhibiting antibiotics confers resistance to antibiotics. *Sci Rep* 6: 28628, 2016.

185. Yukl ET, Elbaz MA, Nakano MM and Moenne-Loccoz P. Transcription Factor NsrR from *Bacillus subtilis* senses nitric oxide with a 4Fe-4S Cluster. *Biochemistry* 47: 13084-1302, 2008.

186. Zhang B, Crack JC, Subramanian S, Green J, Thomson AJ, Le Brun NE and Johnson MK. Reversible cycling between cysteine persulfide-ligated [2Fe-2S] and cysteine-ligated [4Fe-4S] clusters in the FNR regulatory protein. *Proc Natl Acad Sci U S A* 109: 15734-15739, 2012.

187. Zhang DL, Ghosh MC and Rouault TA. The physiological functions of iron regulatory proteins in iron homeostasis - an update. *Front Pharmacol* 5: 124, 2014.

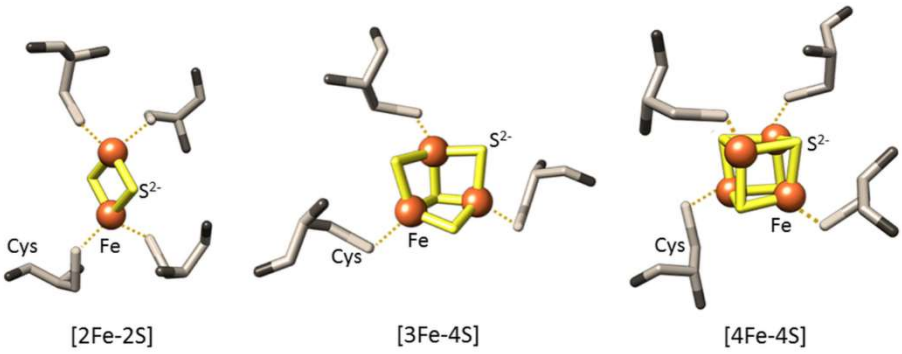

Figure 1

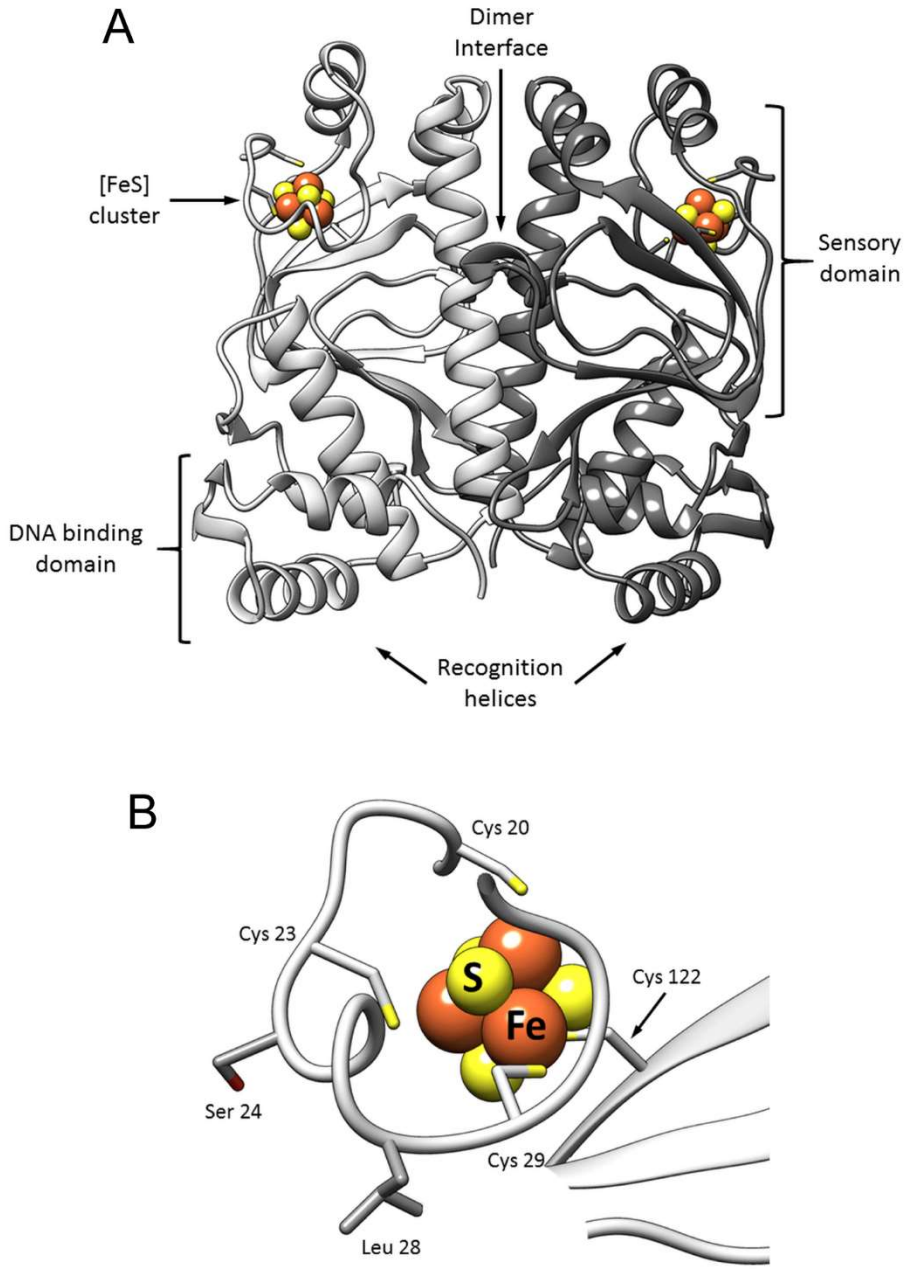
A
Dimer
Interface
[FeS]
cluster
Sensory
domain
DNA binding
domain
Recognition
helices
B
Cys 20
Cys 23
S
Fe
Cys 122
Ser 24
Cys 29
Leu 28

Figure 2

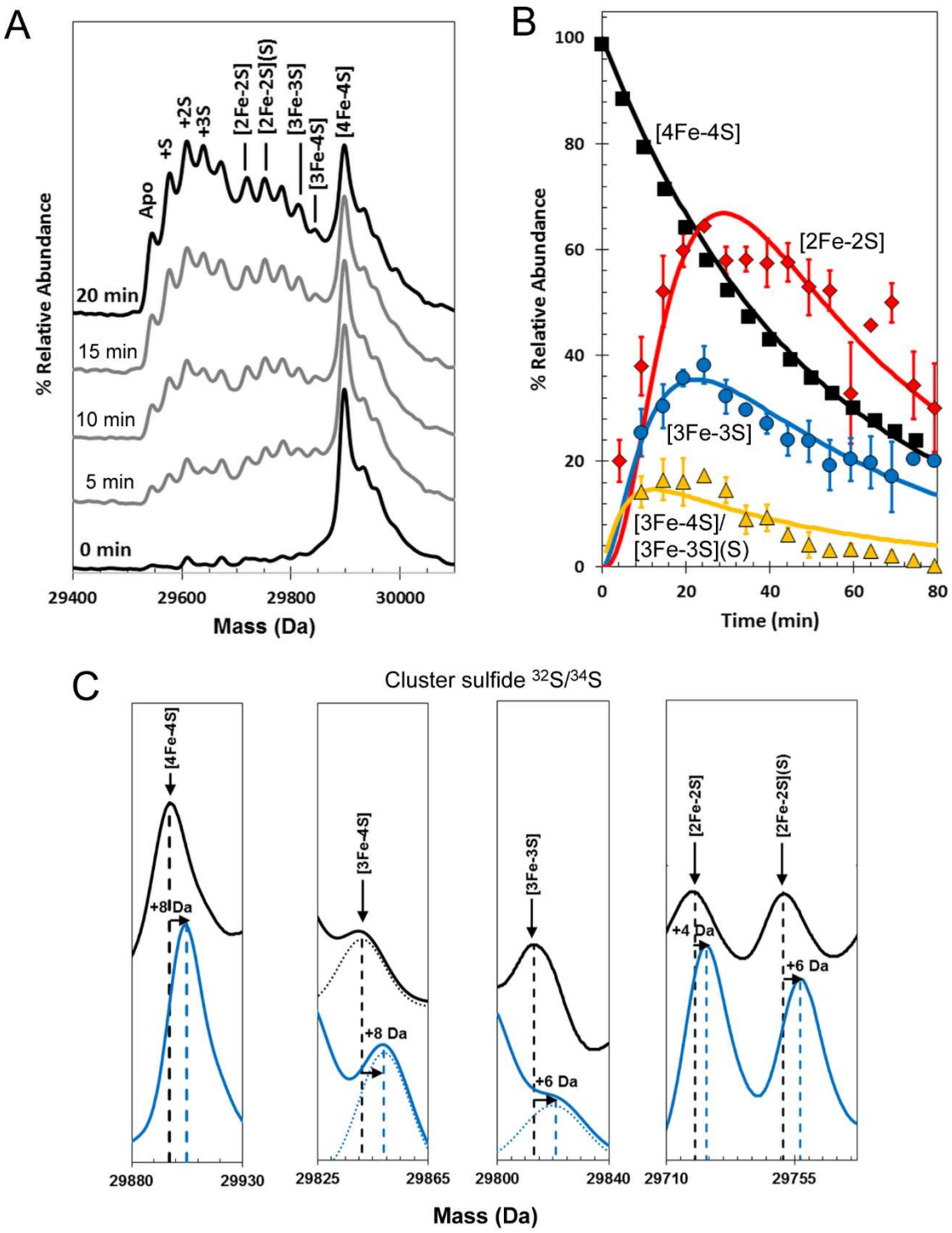
A
% Relative Abundance
Apo
+S
+2S
+3S
[2Fe-2S]
[2Fe-2S](S)
[3Fe-3S]
[3Fe-4S]
[4Fe-4S]
20 min
15 min
10 min
5 min
0 min
29400
29600
29800
30000
Mass (Da)
B
% Relative Abundance
[4Fe-4S]
[2Fe-2S]
[3Fe-3S]
[3Fe-4S]/
[3Fe-3S](S)
0
20
40
60
80
100
Time (min)
C
Cluster sulfide 32S/34S
[4Fe-4S]
+8 Da
[3Fe-4S]
+8 Da
[3Fe-3S]
+6 Da
[2Fe-2S]
+4 Da
[2Fe-2S](S)
+6 Da
29880
29930
29825
29865
29800
29840
29710
29755
Mass (Da)

Figure 3

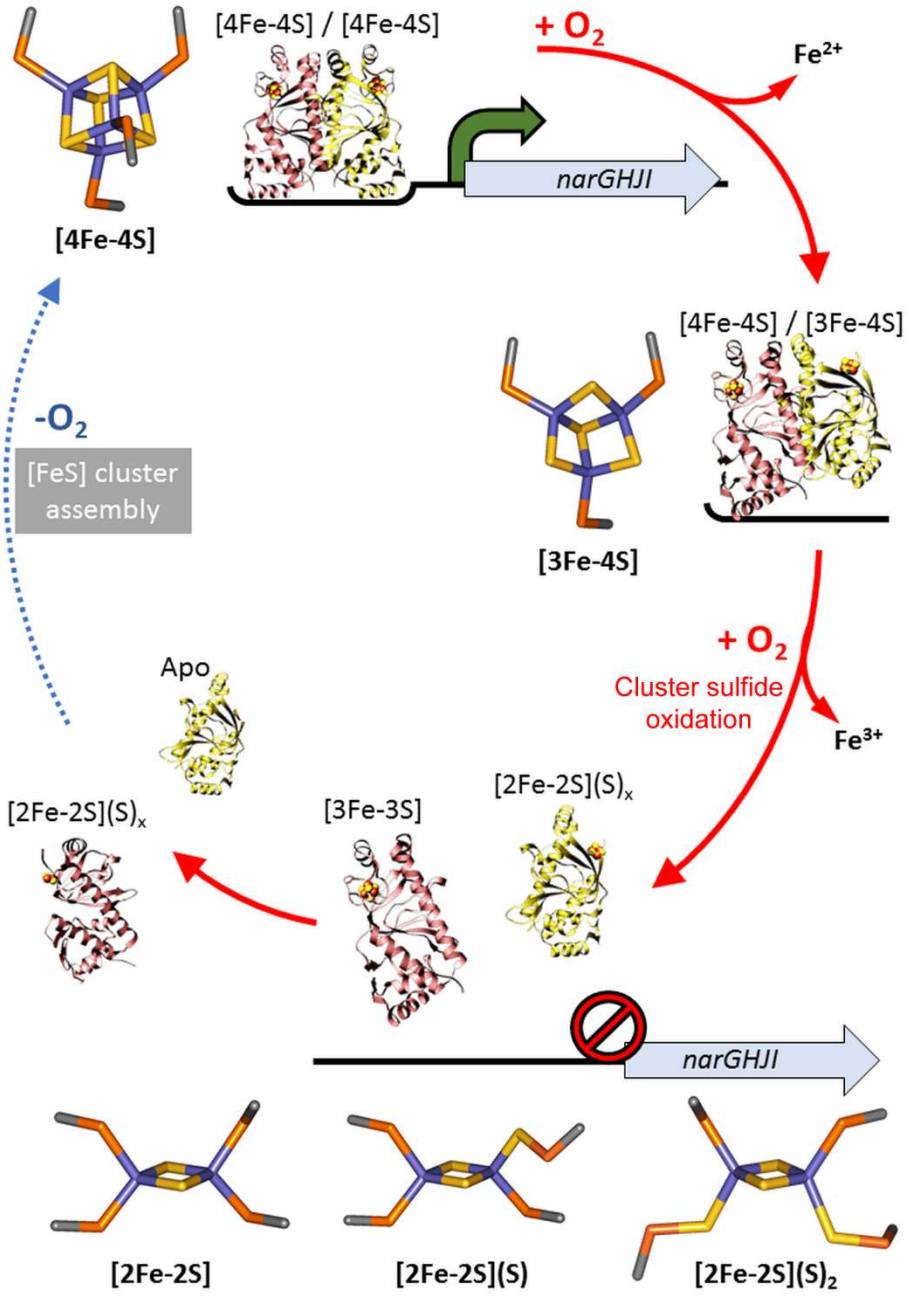
[4Fe-4S] / [4Fe-4S]
+ O2
Fe2+
narGHJI
[4Fe-4S]
[4Fe-4S] / [3Fe-4S]
-O2
[FeS] cluster assembly
[3Fe-4S]
+ O2
Cluster sulfide oxidation
Fe3+
Apo
[2Fe-2S](S)x
[3Fe-3S]
[2Fe-2S](S)x
narGHJI
[2Fe-2S]
[2Fe-2S](S)
[2Fe-2S](S)2

Figure 4

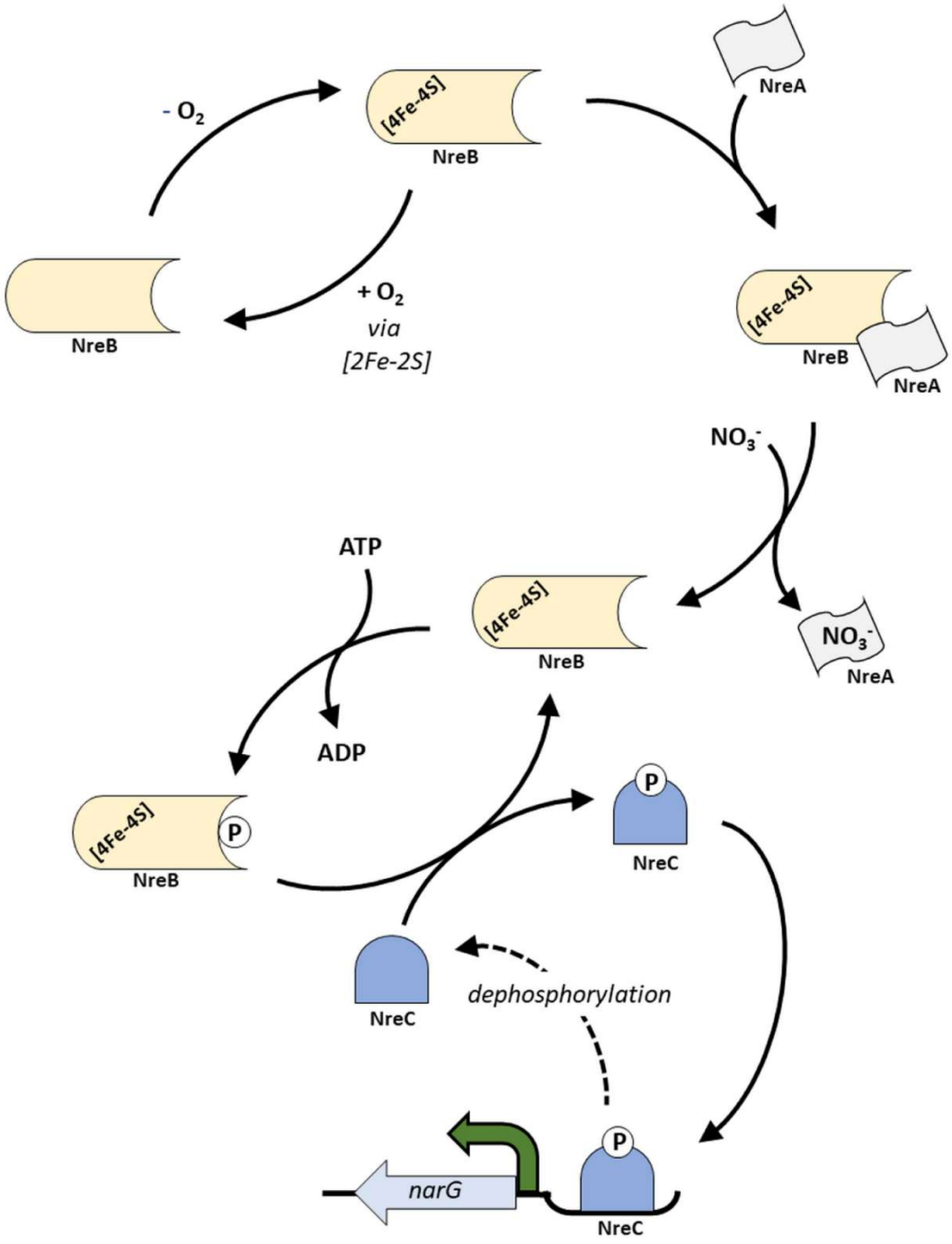
- O2
[4Fe-4S]
NreB
NreA
NreB
+ O2
via
[2Fe-2S]
[4Fe-4S]
NreB
NreA
NO3-
ATP
[4Fe-4S]
NreB
NO3-
NreA
ADP
[4Fe-4S]
P
NreB
P
NreC
NreC
dephosphorylation
narG
P
NreC

Figure 5

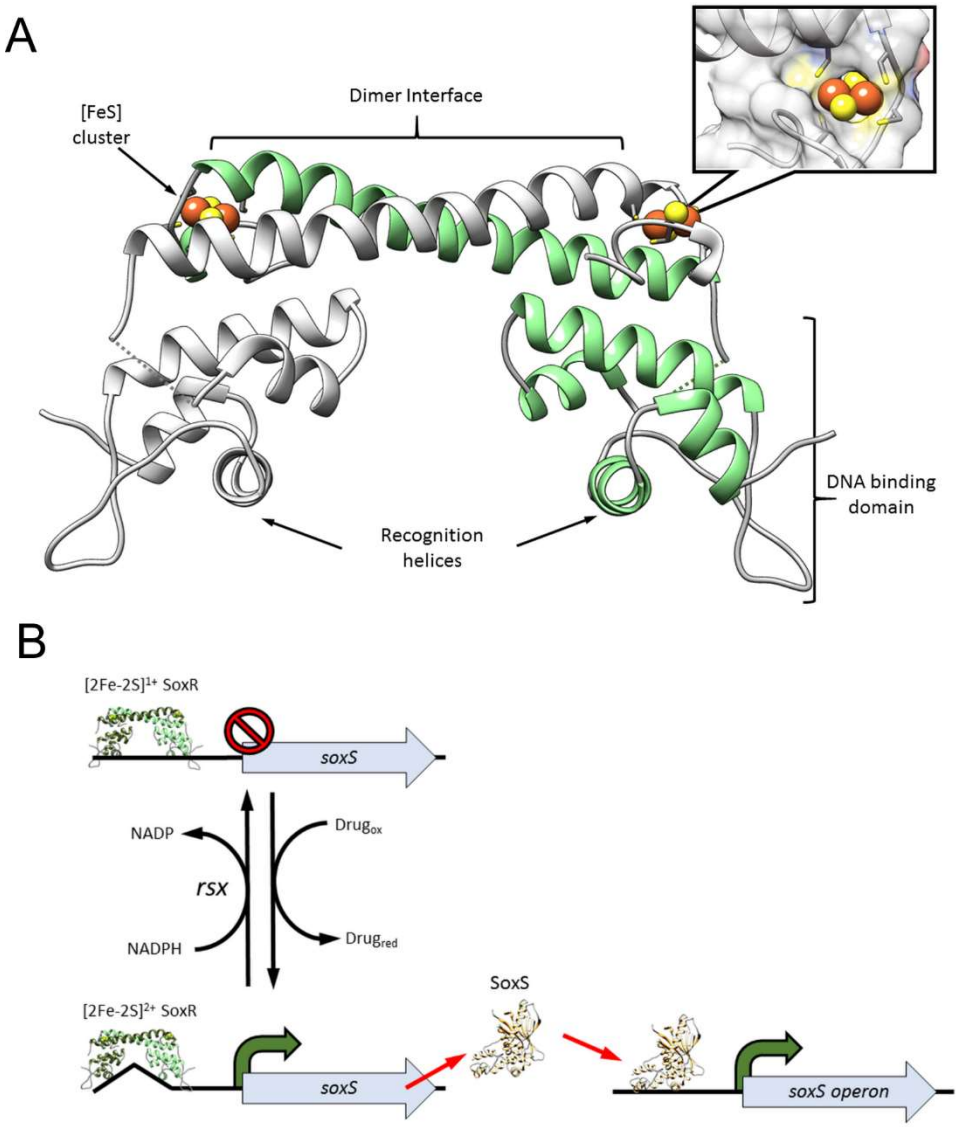
A
[FeS]
cluster
Dimer Interface
DNA binding
domain
Recognition
helices
B
[2Fe-2S]1+ SoxR
soxS
NADP
Drugox
rsx
NADPH
Drugred
SoxS
[2Fe-2S]2+ SoxR
soxS
soxS operon

Figure 6

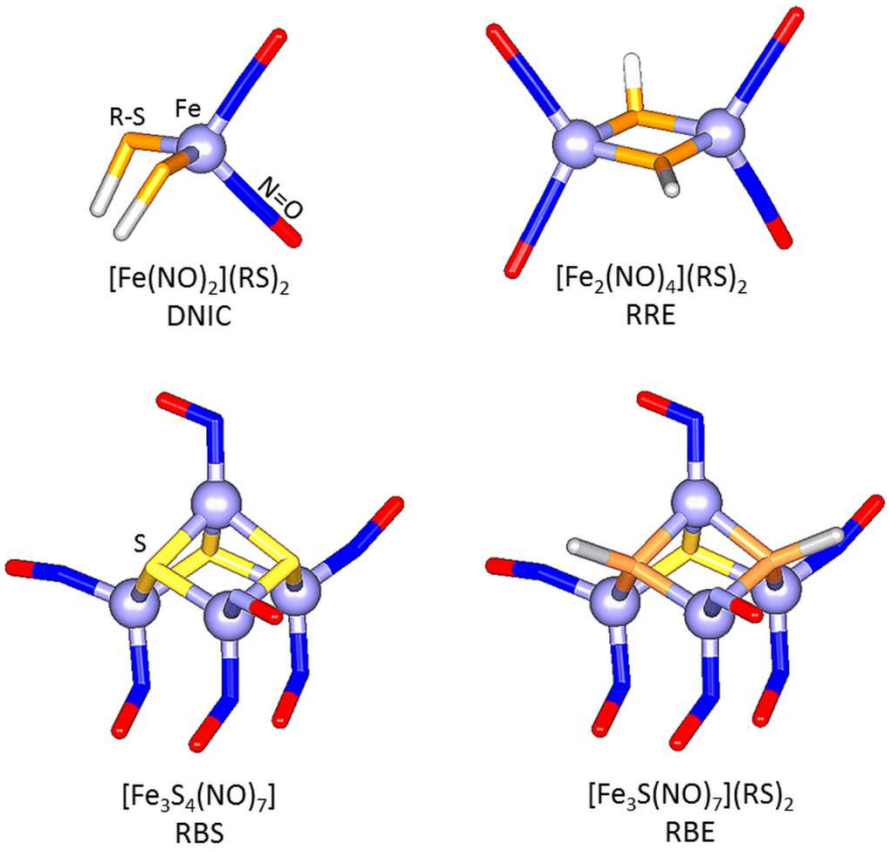
R-S
Fe
N=O
[Fe(NO)2](RS)2
DNIC
[Fe2(NO)4](RS)2
RRE
S
[Fe3S4(NO)7]
RBS
[Fe3S(NO)7](RS)2
RBE

Figure 7

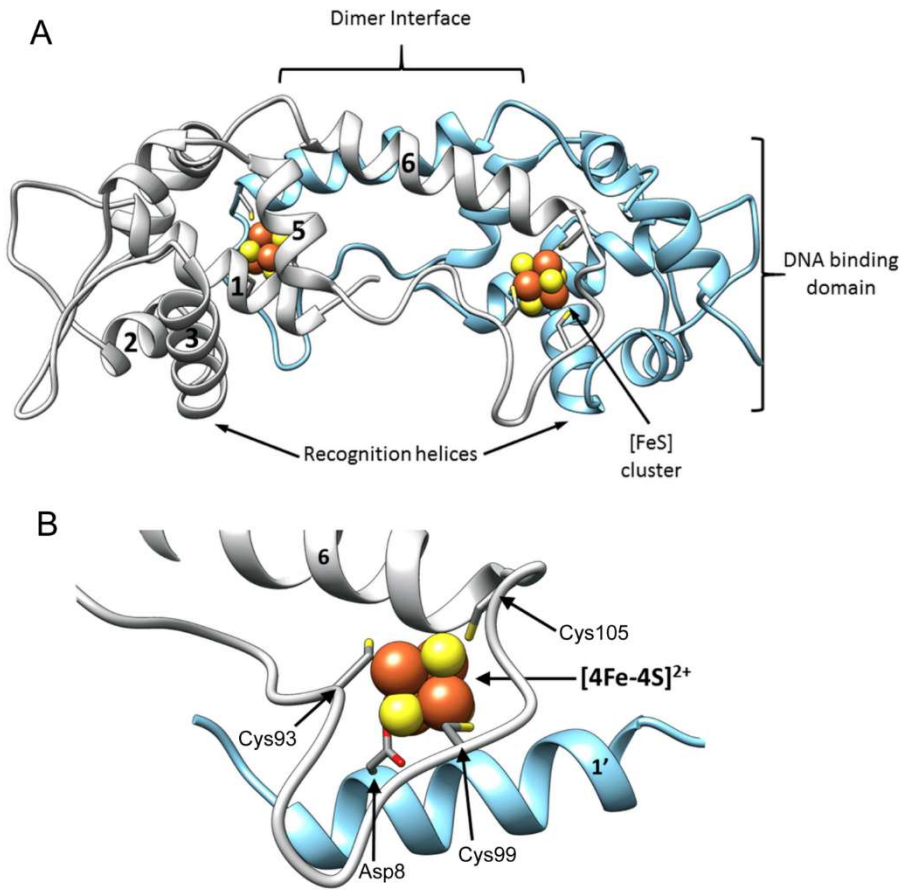
A
Dimer Interface
6
5
1'
2
3
DNA binding
domain
Recognition helices
[FeS]
cluster
B
6
Cys105
[4Fe-4S]2+
Cys93
1'
Asp8
Cys99

Figure 8

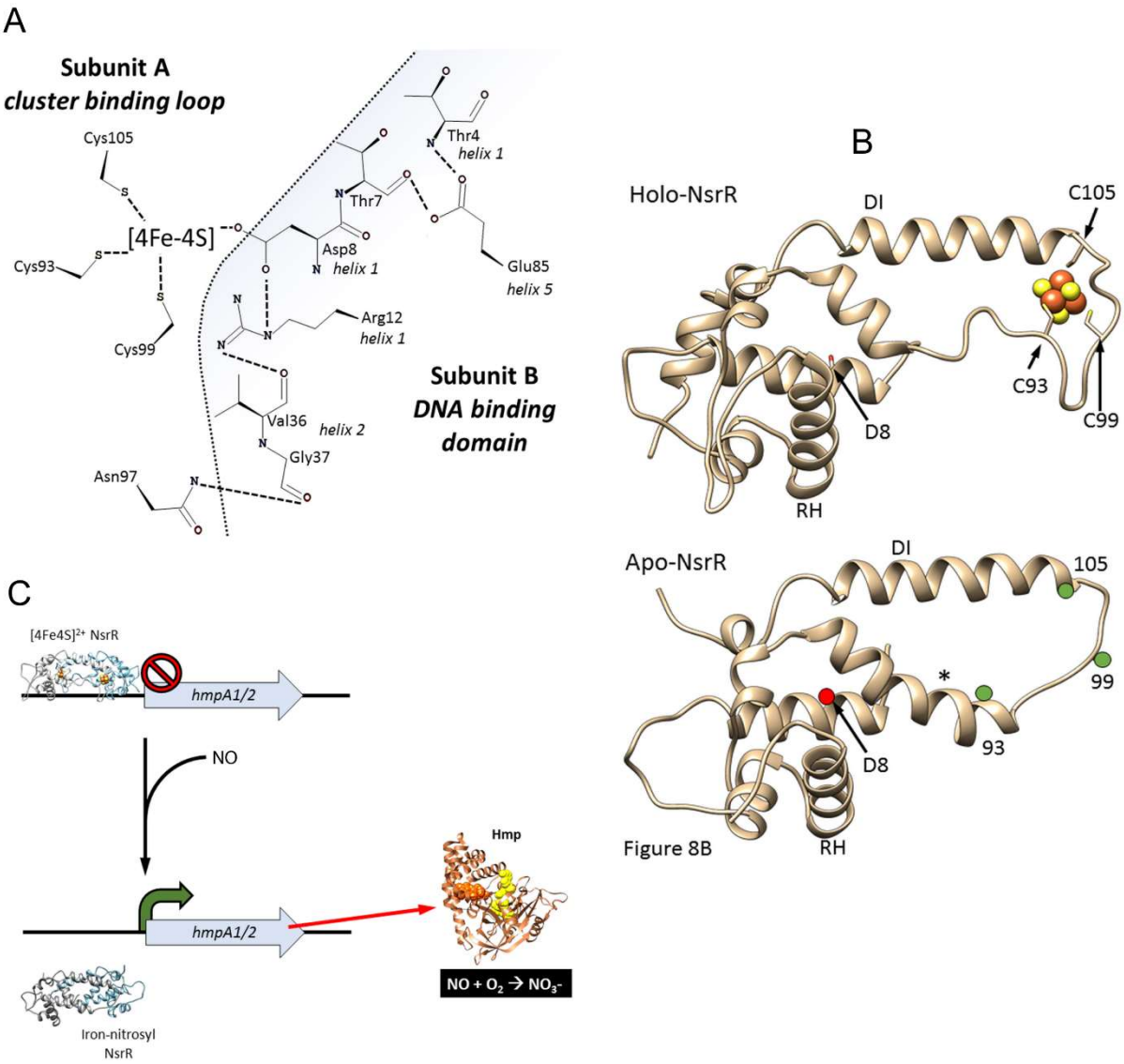

Figure 8B

Figure 9